

Design, Modeling and Analysis of a New Protection Scheme for Type 4 Wind Turbines

A Thesis

Presented in Partial Fulfillment of the Requirements for the

Degree of Master of Science

with a

Major in Electrical Engineering

in the

College of Graduate Studies

University of Idaho

by

Shashidhar Reddy Sathu

Major Professor: Brian K. Johnson, Ph.D.

Committee Members: Herbert Hess, Ph.D.; Ahmed Abdel-Rahim, Ph.D.

Department Administrator: Mohsen Guizani, Ph.D.

December 2016

**Authorization to Submit Thesis**

This thesis of Shashidhar Reddy Sathu, submitted for the degree of Master of Science with a major in Electrical Engineering and titled "Design, Modeling and Analysis of a New Protection Scheme for Type 4 Wind Turbines," has been reviewed in final form. Permission, as indicated by the signatures and dates given below, is now granted to submit final copies to the College of Graduate Studies for approval.

Major  
Professor: \_\_\_\_\_ Date: \_\_\_\_\_  
Brian K. Johnson, Ph.D.

Committee  
Members: \_\_\_\_\_ Date: \_\_\_\_\_  
Herbert Hess, Ph.D.

\_\_\_\_\_  
Ahmed Abdel-Rahim, Ph.D.

Department  
Administrator: \_\_\_\_\_ Date: \_\_\_\_\_  
Mohsen Guizani, Ph.D.

**Abstract**

The short circuit behavior of the early generation wind turbines depends solely on the physical characteristics of the machine. The conventional protection schemes for weak sources can be applied to provide protection to those wind farms. But the full converter based Type 4 Wind turbine generators have complex fault current characteristics which are governed by the converter controls. The control response of the WTGs during fault is not similar to that of synchronous generators. The use of relays with conventional protection schemes may cause misoperation.

In this thesis an attempt is made to explain the complex converter controls and operation and the various grid codes that the wind farms are expected to follow. A new protection scheme is designed based on the system operation and tested with simulation of fault responses of a Type 4 wind turbine in a real time digital simulator. This thesis also explains the reasons that cause misoperation for using convention protection schemes.

## **Acknowledgements**

I wish to express my heartfelt gratitude to my advisors *Dr. Normann Fischer* and *Dr. Brian K Johnson*, who supported me in all the possible ways.

I am also thankful to *Dr. Herbert Hess* who made himself available to clarify my doubts even in the late evenings.

I feel this is the best place to express my regards to the staff of ECE department, University of Idaho, *Mollyann Jones* and *John Jacksha* for their support with logistics, troubleshooting and advice.

*"Dedicated to my mother Swetha Sathu who constantly believed in me, provided moral support and without whom this is not possible."*

## Table of Contents

Authorization to Submit Thesis.....	ii
Abstract.....	iii
Acknowledgements.....	iv
Dedication.....	v
Table of Contents .....	vi
List of Figures .....	x
List of Tables.....	xiv
Acronyms .....	xv
Chapter 1 – Objective and Background .....	1
1.1 Objective.....	1
1.2 Wind Energy.....	3
1.3 WTG – Turbine and dynamics .....	4
1.3.1 Angle of attack.....	7
1.3.2 Tip Speed Ratio .....	9
1.3.3 Calculation of Power Generated from a Wind Turbine .....	10
1.4 Types of Wind Turbine Generators.....	12
1.4.1 Type 1 WTG .....	15
1.4.2 Type 2 WTG .....	16
1.4.3 Type 3 WTG .....	17
1.4.4 Type 4 WTG .....	19
1.5 Need for protection of WTGs .....	22
1.6 What sets this research apart?.....	23
1.7 Overview of the Thesis.....	23

1.8 Summary.....	24
Chapter 2 – Grid Codes .....	26
2.1 The typical requirements for grid connection .....	26
Chapter 3 – Modeling of Type 4 WTG .....	29
3.1 Objective .....	29
3.2 Simulation Software- RSCAD/RTDS .....	29
3.3 Wind Turbine Power Circuit Model .....	29
3.4 Controller Design and Control Aspects.....	37
3.5 Park’s transformation.....	38
3.6 Outer Control Loop.....	41
3.7 Inner Current Control Loop .....	43
3.8 Summary.....	49
Chapter 4 – Converter Model Testing and Simulation Results for Normal Operation ....	50
4.1 Introduction .....	50
4.2 The voltage at the inverter terminals.....	50
4.3 Current Regulator Response.....	51
4.4 Voltages and Currents at Point of Interconnect .....	51
4.5 Voltages and currents at Machine terminals.....	52
4.6 Summary.....	56
Chapter 5 – Fault Analysis .....	57
5.1 Introduction .....	57
5.2 Fault Response Simulation Cases.....	59
5.2a Event 1A: Single Line to Ground Fault (SLG).....	59
5.2b Event 1B: Line to Line Fault (LL) .....	62
5.2c Event 1C: Double Line to Ground fault (DLG).....	65

5.2d Event 2: Three phase fault at 50% of the line .....	68
5.3 Conclusions Drawn.....	72
5.4 Summary.....	72
Chapter 6 – Response of Existing Protection Schemes and Protection Limitations.....	73
6.1 Introduction .....	73
6.2 Overcurrent relay.....	73
6.3 Under Voltage Relay.....	74
6.4 Differential Relay.....	75
6.5 Distance Relay .....	76
6.6 Summary.....	78
Chapter 7 – Proposed Protection Scheme.....	79
7.1 Introduction .....	79
7.2 New Protection Scheme.....	79
7.3 Simulation Results .....	81
7.4 Impact of Fault Location and Fault Resistance.....	85
7.5 Summary.....	86
Chapter 8 – Summary, Conclusions and Future Work .....	87
8.1 Summary.....	87
8.2 Conclusions.....	87
8.3 Future Work.....	89
Appendix A – Test System Component Parameters .....	91
A.1 Permanent Magnet Synchronous Machine (PMSM) ratings .....	91
A.2 Permanent Magnet Synchronous Machine Parameters.....	91
A.3 Diode Bridge Rectifier.....	92
A.4 DC link capacitors .....	92

A.5 NPC Converter.....	93
A.6 Low Pass Filter.....	93
A.7 Transformer.....	94
A.8 Turbine Data.....	95
A.9 Controller.....	95
A.9a High Pass Filter – Control Circuit.....	95
A.9b Compensator.....	97
A.10 Carrier signal.....	98
References.....	99

## List of Figures

Figure 1.1: Horizontal axis wind turbine system [10].....	4
Figure 1.2: Cross section of a wind turbine blade [10] .....	5
Figure 1.3: Turbine blade cross section with wind direction.....	5
Figure 1.4: Turbine blade – Bernoulli’s principle [10].....	6
Figure 1.5: Turbine cross section, angle of attack and forces acting [10].....	7
Figure 1.6: Separation of wind with higher angle of attack .....	8
Figure 1.7: Lift force as a function of angle of attack [10].....	8
Figure 1.8: TSR – Wind turbine .....	9
Figure 1.9: Mechanical power output for different rotor speeds and wind speeds.....	10
Figure 1.10: B-H Curve of an Iron Core .....	13
Figure 1.11: B-H Curve of a Magnetic Core Ignoring Hysteresis .....	14
Figure 1.12: Schematic Circuit Diagram of a Type 1 Wind Turbine Generator .....	15
Figure 1.13: torque – speed and pf – speed characteristics of an induction machine .....	16
Figure 1.14: Schematic Circuit Diagram of Type 2 Wind Turbine Generator.....	17
Figure 1.15: Schematic Circuit diagram of Type 3 wind turbine generation .....	18
Figure 1.16: Permanent Magnet Synchronous Machine.....	20
Figure 1.17: Schematic circuit diagram of Type 4 PMSM wind turbine generator .....	21
Figure 1.18: Squirrel cage induction machine and converter structure in Type 4 WTG	22
Figure 2.1: Typical grid voltage magnitude requirements [2] .....	28
Figure 3.1: Diode bridge rectifier – simulation model .....	30
Figure 3.2: 2 Level Voltage Source Converter.....	31
Figure 3.3: Output of two level converter – phase to phase voltage.....	31
Figure 3.4: T type, 3 level converter .....	32

Figure 3.5: NPC type, 3 level converter .....	32
Figure 3.6: Phase to phase output of a 3 level converter .....	33
Figure 3.7: Simulation Model – Three phase, three level NPC converter.....	34
Figure 3.8: ‘A’ phase leg of a 3 level NPC converter.....	35
Figure 3.9: Schematic diagram of sine triangle PWM with unipolar triangular wave .....	35
Figure 3.10: Schematic diagram of a PWM scheme for 3 level NPC converter [1] .....	36
Figure 3.11: Circuit diagram of L and LCL filters.....	37
Figure 3.12: dq0 transformation of 3 phase quantities .....	39
Figure 3.13: Time domain representation of dq0 transformation .....	40
Figure 3.14: Simulation blocks (a) ABC – dq0, (b) dq0 - ABC.....	41
Figure 3.15: generic power flow diagram of AC/DC/AC converter. ....	42
Figure 3.16: Control model of outer control loop .....	43
Figure 3.17: Phase ‘A’ Circuit representation of converter, filter and transformer .....	44
Figure 3.18: Control model of the loop equation [1].....	45
Figure 3.19: Control block diagram of the converter system .....	46
Figure 3.20: Simulation model - ID and IQ current regulator .....	48
Figure 3.21: Test system diagram .....	48
Figure 4.1: Terminal voltage of the inverter–A phase over(A)10 cycles and(B)1 cycle .	50
Figure 4.2: Id Iq reference and measured values .....	51
Figure 4.3A: Voltages at the Point of Interconnect.....	52
Figure 4.3B: Currents at the Point of Interconnect.....	52
Figure 4.4: Single phase full wave rectifier.....	53
Figure 4.5: Input and output of a 1 $\phi$ full wave rectifier .....	53
Figure 4.6: Comparison of In/Out of 1 $\phi$ full wave rectifier with capacitor on DC side...	54
Figure 4.7: Voltage waveforms at the PMSM terminals.....	55

Figure 4.8: Current in the AC side for a 1 $\phi$ full wave rectifier .....	55
Figure 4.9: Currents at PMSM terminals.....	56
Figure 5.1: Type 4 WTG simulation test system with fault.....	57
Figure 5.2: Line to ground voltages at relay location - Event 1A .....	59
Figure 5.3: Phase currents at relay location – Event 1A .....	60
Figure 5.4: Fault current – Event 1A .....	60
Figure 5.5: DC link voltage – In each capacitor branch (in per unit) – Event 1A.....	61
Figure 5.6: Crowbar current for SLG fault.....	61
Figure 5.7: Line to ground voltages at relay location– Event 1B.....	62
Figure 5.8: Phase currents at relay location – Event 1B .....	62
Figure 5.9: Fault current – Event 1B.....	63
Figure 5.10: DC link voltage – In each capacitor branch (in per unit) – Event 1B.....	64
Figure 5.11: Crowbar current – Event 1B.....	64
Figure 5.12: Line to ground voltages at relay location – Event 1C .....	65
Figure 5.13: Phase currents at relay location – Event 1C.....	66
Figure 5.14: Fault current – Event 1C.....	66
Figure 5.15: DC link voltage – in each capacitor branch (in per unit) – Event 1C .....	67
Figure 5.16: Crowbar current – Event 1C.....	68
Figure 5.17: Line to ground voltages at relay location – Event 2 .....	69
Figure 5.18: Phase currents at relay location – Event 2 .....	69
Figure 5.19: Fault currents – Event 2.....	70
Figure 5.20: DC link voltage – in each capacitor branch (in per unit) – Event 2.....	71
Figure 5.21: Crowbar current – Event 2 .....	71
Figure 6.1: Impedance Relay Characteristic.....	77
Figure 7.1: Type 4 WTG simulation test system with fault.....	80

Figure 7.2: Calculated RMS voltage magnitude at the relay location – Event 1A.....	81
Figure 7.3: Calculated RMS voltage magnitude at the relay location – Event 1B.....	82
Figure 7.4: Calculated voltage magnitude at the relay location – Event 1C .....	83
Figure 7.5: Calculated voltage magnitude at the relay location – Event 2.....	84
Figure 7.6: Length of line to the fault point versus Modulating wave magnitude.....	85

**List of Tables**

Table 7.1: Modulating wave magnitude for different fault length, $R_f=0$ .....	85
Table A.1: Wind turbine (PMSM) generator ratings .....	91
Table A.2: Wind turbine (PMSM) generator per unit parameters[3].....	91
Table A.3: Rectifier – diode ratings.....	92
Table A.4: DC link capacitor values.....	92
Table A.5: NPC converter switch ratings .....	93
Table A.6: L filter values.....	94
Table A.7: Transformer ratings .....	94
Table A.8: Turbine Data.....	95

## **Acronyms**

**CT** – Current Transformer

**CTR** – Current Transformer Ratio

**DFIG** – Doubly Fed Induction Generator

**DLG** – Double Line Ground

**EMF** – Electro Motive Force

**GB** – Gear Box

**GSC** – Grid Side Converter

**IEEE** – Institute of Electrical and Electronics Engineers

**KE** – Kinetic Energy

**KVL** – Kirchhoff's Voltage Law

**LL** – Line to Line Fault

**LVRT** – Low Voltage Ride Through

**PF** – Power Factor

**PI** – Proportional Integral

**PMSG** – Permanent Magnet Synchronous Generator

**PTR** – Potential Transformer Ratio

**PWM** – Pulse Width Modulation

**RPM** – Revolutions Per Minute

**RTDS** – Real Time Digital Simulator

**RSCAD** – RTDS Simulator Computer Aided Design

**SCIG** – Squirrel Cage Induction Generator

**SLG** – Single Line to Ground

**SG** – Synchronous Generator

**TSR** – Tip Speed Ratio

**VSC** – Voltage Source Converter

**VT** – Voltage Transformer

**WRIG/M** – Wound Rotor Induction Generator/Machine

**WT** – Wind Turbine

**WTG** – Wind Turbine Generator

**WTS** – Wind Turbine System

## **Chapter 1 – Objective and Background**

### **1.1 Objective**

The rapid increase of energy demand globally and the impending threat of the extinction of fossil fuel reserves is forcing the world to switch to other sources of energy. Switching to renewable energy sources provides substantial benefits for climate, health and economy. Keeping this in view many governments changed policies with the intention to expand the use of rapidly growing renewable energy technologies. The growth of renewable energy technologies has led to the increase in penetration of wind turbine generators (WTG) in power systems.

The development of the WTG technologies led to online grid connections of wind turbines, which is a switch from the older offline generation. Almost all new megawatt scale wind power plants that are being developed use either variable speed doubly fed induction generators (Type 3) or full converter based (Type 4) WTGs [11].

Type 3 and Type 4 WTGs can be used to produce energy over a wide range of wind speeds. They allow fast and independent control of active and reactive power. They have the capability of limiting the fault current contributions and at the same time are also able to comply with low voltage ride through (LVRT) requirements set forth by industry regulatory agencies. Due to the interconnection of wind turbines to the grid, it is important to study their short circuit behavior to design and implement an adequate protection system to make the system safer, more reliable and easier to operate.

Generally short circuit studies are done to determine the settings for protection schemes to adopt for the part of the power system under study. The Type 1 WTGs are

fixed speed squirrel cage induction machines and Type 2 WTGs employ variable slip wound rotor induction machines. The short circuit behavior of Type 1 and Type 2 WTGs are dependent on physical characteristics of the WTGs which are dominated by transient and sub-transient impedances, and are well understood. The fault current contributions for such WTGs are determined by the physics (construction) of the machines. The fault current can be several times the rated current for a fault near the WTG terminals. The fault current is limited by the system and the WTG impedances.

But, on the other hand, Type 3 and Type 4 WTGs have much more complex fault current characteristics. The fault current characteristics are governed by the proprietary controls of the converters used in the generators. Since the Type 4 WTG is fully converter based, the fault current is limited to 1.1 to 1.2 times the rated load current. The short circuit characteristics of Type 3 WTGs are similar to those of Type 4 WTGs, the only difference being the crow bar operation during severe faults. During the crow bar operation of a DFIG the fault characteristics follows a transition from a controlled current source to that of a conventional induction generator.

The relatively nascent nature of Type 3 and Type 4 WTGs makes design of protection schemes difficult because the existing tools do not accurately model the dynamics of these WTG control systems. The true fault behavior of the system is required to design a reliable method from a protection perspective. The manufacturers control schemes are confidential and proprietary. The Type 4 WTG modifies the waveforms to limit the current magnitude and balances the currents during the disturbances. This unconventional behavior of the Type 4 WTG presents a host of challenges for designing reliable protection schemes.

Over many years, the power industry has developed many methods for modeling various WTGs and their associated control systems. Initiatives have been organized by Western Electricity Coordinating council (WECC), Institute of Electrical and Electronics Engineers (IEEE) and International Electro-technical Commission (IEC) working groups to develop generic models for various WTG types. However, the generic models developed are identified as not being suitable for fault studies [11].

In this research, an absolute model of a Type 4 WTG is developed in order to simulate the fault behavior of the wind turbine. A study is done to check whether the present protection schemes can be used and what their limitations are. The limitations for employing those schemes are identified and presented. A new protection scheme is then designed based on the WT system operation and verified for different faults.

## **1.2 Wind Energy**

The velocity of the wind or, in other words, kinetic energy contained in the air is the basic source of wind power generation. There are various factors that are responsible for the origination of the wind [18]. The factors that constitute a major role are

- Movement of earth (rotation of earth)
- Uneven heating of the atmosphere
- Irregularities of the earth's surface

This kinetic energy in wind is harvested into useful electrical energy by means of wind turbine generators. The conversion of kinetic energy to electrical energy has an intermediate stage of mechanical energy. The kinetic energy of wind is converted to

mechanical energy by means of a turbine and this energy is then converted to electrical energy by means of a generator.

### 1.3 WTG – Turbine and dynamics

Wind turbines are generally classified into two basic types based on the axis of rotation. The turbines that are designed to rotate on a horizontal axis are called Horizontal axis wind turbines and the turbines that rotate on a vertical axis are called Vertical axis wind turbines.

Wind turbine (WT) is a generic phrase given to the wind energy system that converts wind into electrical energy [10]. The present power ratings of wind turbines range from 50kW to 8MW. The most efficient types of turbines are horizontal axis wind turbine. A general structure of a horizontal axis turbine is shown in Figure 1.1.

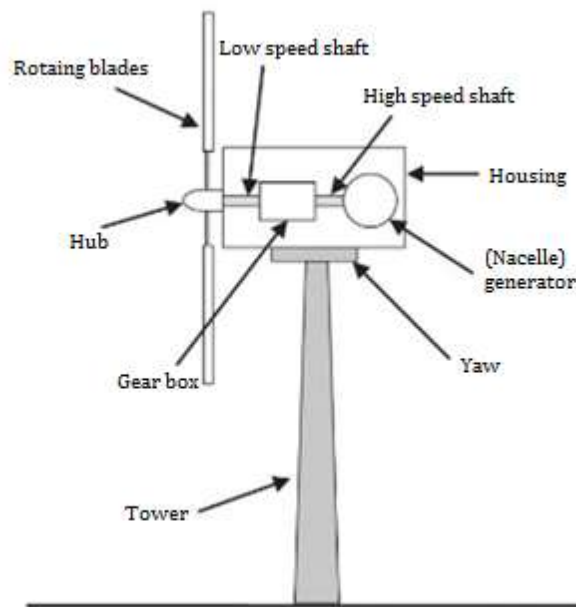


Figure 1.1: Horizontal axis wind turbine system [10]

The blade structure is the main element in capturing the kinetic energy from the wind and converting it into rotational energy. It behaves similar to wing of an aircraft. The cross section of the blade forms an airfoil as shown in Figure 1.2. The cross sectional view is has two cambers (arcs), an upper arc and a lower arc. The upper arc is longer than the lower arc, this is a key design feature which is responsible for the movement of the turbine blades. The edge that faces towards the wind is called the leading edge and the other the trailing edge. The straight line connecting the leading edge to the trailing edge is often termed as the chord line.

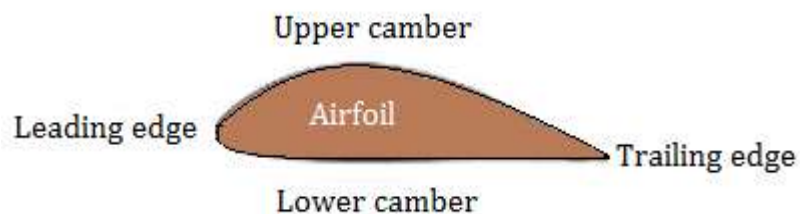


Figure 1.2: Cross section of a wind turbine blade [10]

The interaction of the airfoil with the wind flow is shown in Figure 1.3.

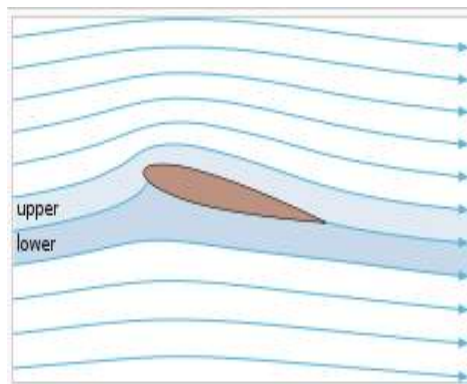


Figure 1.3: Turbine blade cross section with wind direction

When air molecules hit the leading edge of the turbine blade, they split into two paths along the upper camber of the blade and along the lower camber. According to the law of continuity, the air molecules separated at the leading edge meet at the trailing edge at the same time. The paths they follow are of different lengths, but the time is the same for both the paths. The velocity of the air molecules above the turbine blade is larger when compared to that of the molecules in the lower path. Bernoulli's principle states that the pressure decreases as the velocity increases and vice versa. Based on this principle the pressure exerted on the upper ( $P_{r1}$ ) camber is less than the lower camber ( $P_{r2}$ ) as depicted in Figure 1.4. There will be a resultant upward pressure ( $P_{net}$ ) due to this difference in the pressures.

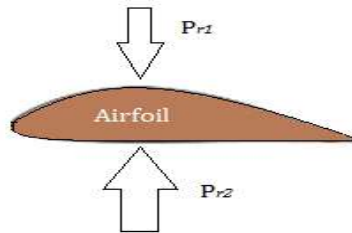


Figure 1.4: Turbine blade – Bernoulli's principle [10]

$$P_{net} = P_{r2} - P_{r1} \quad (1.1)$$

There will be net force ( $F_{net}$ ) acting on the turbine blade associated with the net pressure.

$$F_{net} = P_{net}A \quad (1.2)$$

This force actually has two components; lift force and drag force. The component of force perpendicular to the chord line is lift force, which is responsible for the movement

of the turbine. The component of force along the chord line is drag force which is an unavoidable frictional loss.

### 1.3.1 Angle of attack

The force components can be controlled by changing the angle of attack. An angle of attack ( $\alpha$ ) is the angle between relative direction of wind and the chord line. Since the lift force is the force that is responsible for the movement of turbine blades, it is the major component that has to be examined, as shown in Figure 1.5. The magnitude of lift force increases with the angle of attack.

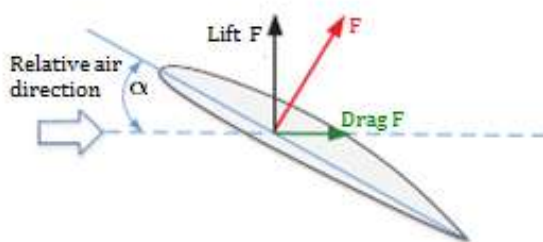


Figure 1.5: Turbine cross section, angle of attack and forces acting [10]

After reaching a certain point the wind flowing along the blade surface in the upper camber separates from the blade and causes turbulence at the trailing edge as shown in Figure 1.6. This is the reason for a stalling condition of the wind turbine. The relative wind direction changes with wind speed, so does the angle of attack. At a wind speed higher than the rated speed, the wind turbines stall. Hence it is generally advised to stop the wind turbine generation if the speed of wind goes beyond a nominal value. The nominal speed of wind is typically 12m/s although this varies slightly with turbine size and construction.

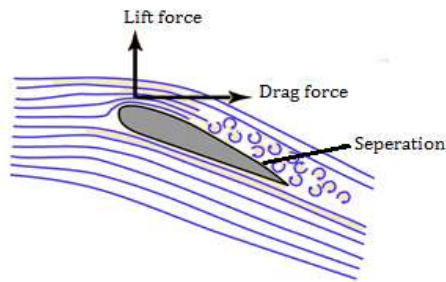


Figure 1.6: Separation of wind with higher angle of attack

The change in lift force magnitude along with the variation of angle of attack is depicted in Figure 1.7.

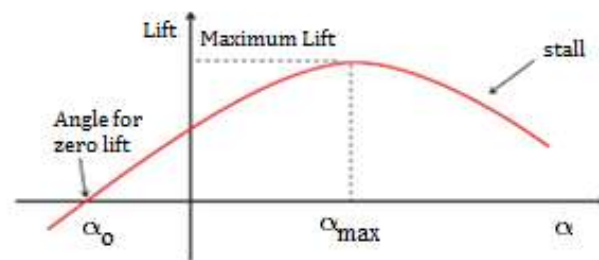


Figure 1.7: Lift force as a function of angle of attack [10]

To convert maximum amount of kinetic energy in the wind to useful mechanical energy, the turbine has to be operated in the optimum condition of lift force. The lift force changes with angle of attack. The relative direction of the wind will be continuously varying and cannot be altered, but it is possible to have the control over the turbine blade alignment with the wind direction. This can be achieved by changing the chord line position. This is possible by means of pitch control i.e., changing the angle of blades mounted on the hub of the turbine with respect to the wind direction with the help of an actuator.

The implementation of a control for operating the turbine at optimum lift force condition will be complex if the control is done directly. To make it simpler, a ratio called Tip Speed Ratio (TSR) is defined.

### 1.3.2 Tip Speed Ratio

The tip speed ratio or TSR for wind turbines is the ratio of the tangential speed at the tip of the turbine blade to the actual wind speed.

$$\lambda = \frac{\text{Tip speed of blade}}{\text{Wind speed}}$$

$$\lambda = \frac{\omega R}{v_w} \quad (1.3)$$

where:  $\lambda$  is tip speed ratio

$\omega$  is the angular velocity of the blade

$R$  is the length of the blade

$v_w$  is the actual wind speed

A clear picture of the quantities is depicted in Figure 1.8. The direction of wind is perpendicular to the swept area of the turbine blades.

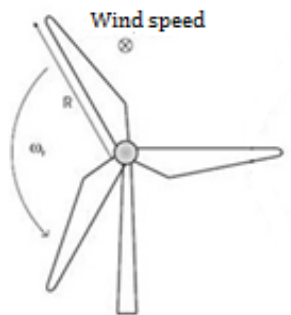


Figure 1.8: TSR – Wind turbine

The tip speed ratio (TSR) is constant for operation of the wind turbine at the optimal condition. This fact is used for the pitch control in order to trap maximum kinetic energy of wind to convert it into useful mechanical energy.

The variation of mechanical energy produced for conversion into electrical energy for various wind speeds and rotor speeds is shown in Figure 1.9.

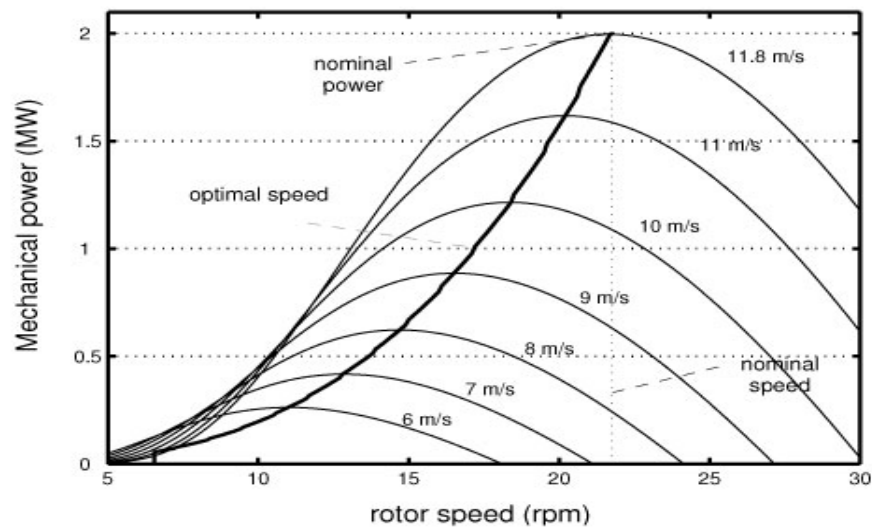


Figure 1.9: Mechanical power output for different rotor speeds and wind speeds

The thick line connects the maximum power at each wind speed for a constant TSR. Turbines are operated at this condition for maximum efficiency.

### 1.3.3 Calculation of Power Generated from a Wind Turbine

The kinetic energy containing in the wind is given by the equation (1.4).

$$KE = \frac{1}{2}mv_w^2 \quad (1.4)$$

Where: KE is kinetic energy of the wind,

m is mass of the fluid (air)

$v_w$  is the velocity of the wind

$$P = \frac{\text{Energy}}{\text{Time}} \quad (1.5)$$

Power is energy per unit time

$$P_{mech} = \frac{d\left(\frac{1}{2}mv_w^2\right)}{dt} \quad (1.6)$$

Where only the mass is varying,

$$P_{mech} = \frac{1}{2}\dot{m}v_w^2 \quad (1.7)$$

And  $\dot{m}$  is the mass flow rate.

The mass ( $m$ ) of a fluid is density ( $\rho$ ) times its volume ( $V$ ), so substituting,

$$\dot{m} = \frac{d(\rho V)}{dt} \quad (1.8)$$

Resubstituting the volume as length times cross sectional area and putting this value in equation (1.7) gives

$$P_{mech} = \frac{1}{2}\rho A \left(\frac{dx}{dt}\right) v_w^2 \quad (1.9)$$

Where  $\frac{dx}{dt}$  is actually the speed of the wind. Therefore,

$$P_{mech} = \frac{1}{2}\rho A v_w^3 \quad (1.10)$$

The amount of energy that can be extracted from the wind is characterized by Betz's law. According to this law no turbine can capture more than 16/27 (59.3%) of the kinetic energy. This is independent of the design of the wind turbine in open flow. The

factor  $16/27$  is called the Betz coefficient. Practically, wind turbines achieve at peak 75-80% of the Betz limit.

$$P_{avail} = \frac{1}{2} C_p \rho A v_w^3 \quad (1.11)$$

where  $C_p$  is the efficiency coefficient

This value of power is available for conversion to electrical energy, which is done by means of electrical machines. Over the course of time the machines used in the wind turbines have changed. A brief discussion of these will follow. For this research, Type 4 wind turbine will be used, with a permanent magnet synchronous machine as the generator in this case.

#### 1.4 Types of Wind Turbine Generators

Wind turbine systems are classified into four types in the order of their development progression

- Type 1 – Squirrel cage induction generator, fixed speed wind turbine
- Type 2 – Wound rotor induction generator, variable speed with rotor resistance
- Type 3 – Doubly fed induction generator, variable speed turbine
- Type 4 – Permanent magnet synchronous generator or squirrel cage induction generator with active machine side converter

Before going into the types of turbines, a brief discussion about electrical machines will be given, including the requirements for the machine to convert mechanical energy provided as torque on the rotor to real power in terms of electrical energy.

A B-H curve of an iron core, as shown in Figure 1.10, shows the relation between the magnetic flux density and magnetic field strength. For every power system cycle of operation it traverses the path bcdefgb. The difference between the path from positive peak to negative peak and from negative peak to positive peak is due to the hysteresis phenomena. The area enclosed by the curve represents the hysteresis loss per cycle of operation.

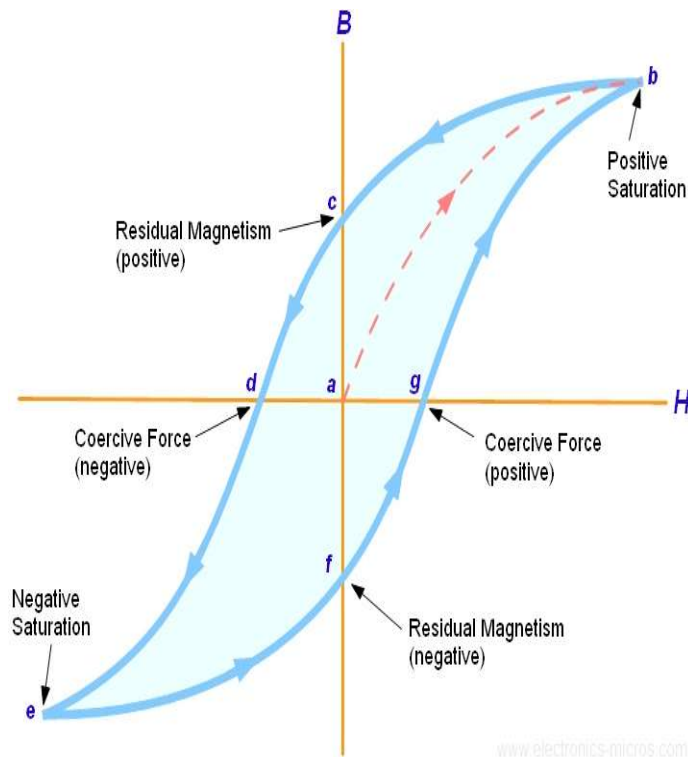


Figure 1.10: B-H Curve of an Iron Core

If one ignores hysteresis, the curve would transform as shown in the Figure 1.11. The slope of the curve gives the magnetic permeability  $\mu$  of the material. The core is operated in the region up to the knee point, where the curve is fairly approximated to be linear.

$$\mu = \frac{\Delta B}{\Delta H} = \frac{B}{H} \quad (1.12)$$

where:  $\mu$  - Magnetic permeability of the core

B – Magnetic Flux density

H – Magnetic field intensity

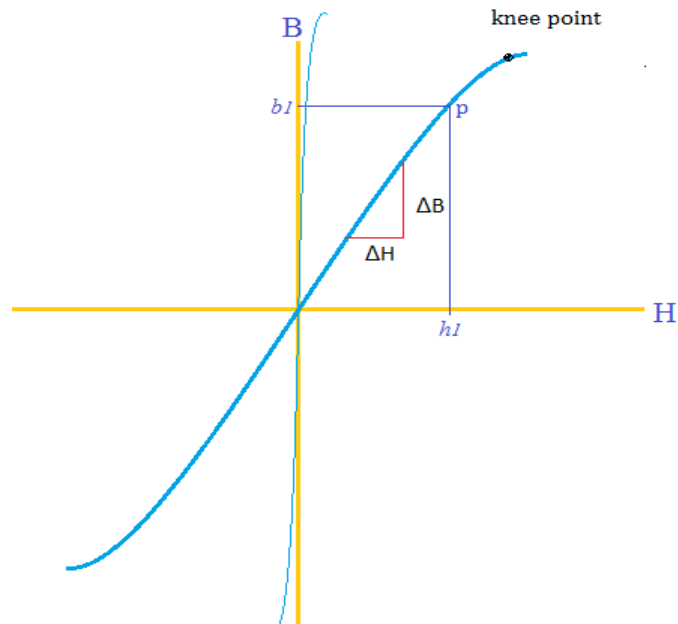


Figure1.11: B-H Curve of a Magnetic Core Ignoring Hysteresis

The point 'p' on the curve, shows that the core requires current corresponding to  $h_1$  to align its domain to provide the flux density  $b_1$ . Ideally the current required by the core is zero and the curve coincides with the B-axis. The slope of this curve is  $\mu = \tan(90^\circ) = \infty$ , and for an ideal core the permeability is infinite. But, for real cores including the core used show this deviation, the slope is finite. As a result of the finite magnetic permeability, the core requires magnetizing current to excite the machine. This current is in phase with the flux but the flux lags the voltage by  $90^\circ$  because of derivative relationship. Hence the current required for exciting the core (magnetizing current) is purely inductive, and consumes reactive power. In order to extract real power from the

generator, reactive power has to be supplied to the system. In the course of evolution of different types of wind turbines, the methods for providing reactive power have changed. The types of generators can be classified based on these differences.

### 1.4.1 Type 1 WTG

Initially wind turbine generators were manufactured using squirrel cage induction machines. In a Type 1 WTG, the terminals of the machine are connected to AC system. The reactive power required by the machine is provided directly through these terminals. In most cases utilities don't want the machines to draw reactive power from the grid as it could affect the voltage stability of the system. So capacitor banks were installed in parallel with the machine terminals to provide reactive power. In order to generate real power, the machine has to operate in super synchronous region i.e., at a rotor speed greater than the synchronous speed for the effective number of poles.

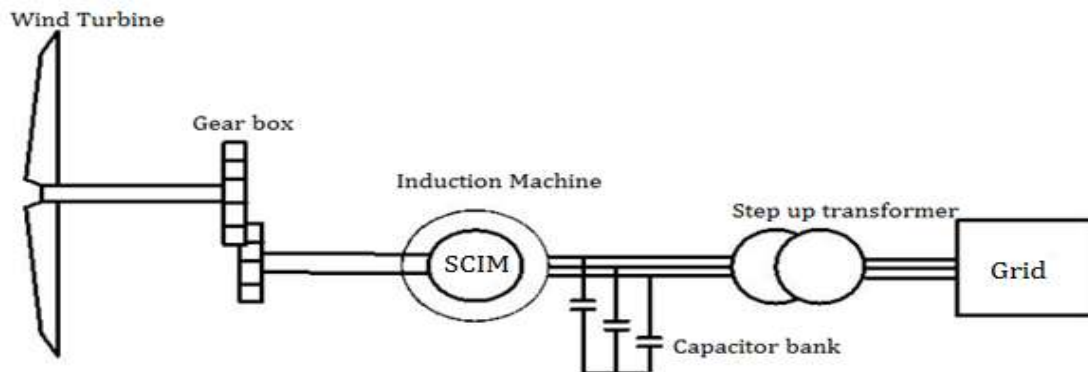


Figure 1.12: Schematic Circuit Diagram of a Type 1 Wind Turbine Generator

The torque-speed and power factor-speed characteristics of the machine are shown in Figure 1.13. In order to keep the machine in generator mode, it has to be in

the generating region. The turbines of this type are to be considered fixed speed wind turbines.

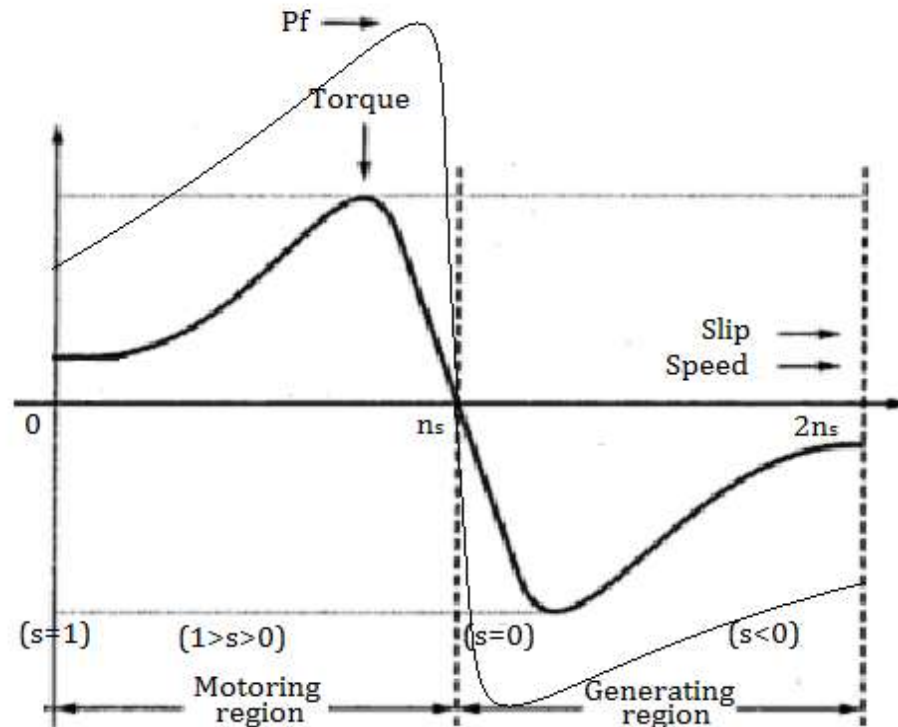


Figure 1.13: torque - speed and pf - speed characteristics of an induction machine

As a result the speed of the turbine rotor is fixed for a particular wind speed. The point of operation is determined solely by the wind speed and the turbine would rarely operate in the optimum power condition.

### 1.4.2 Type 2 WTG

Type 2 wind turbine generators employ a wound rotor induction machine. To get the control over the operating point of the machine the rotor circuit is connected to a set of switched resistors on each phase by means of slip rings. By varying the resistance in the rotor circuit the speed of the machine can be controlled, allowing

operation close to the optimum condition. Other than this, everything else is similar to Type 1 WTG. The Type 2 WTG also requires a capacitor bank to keep the reactive power exchange with the grid close to zero. A schematic circuit of a Type 2 WTG is shown in Figure 1.14.

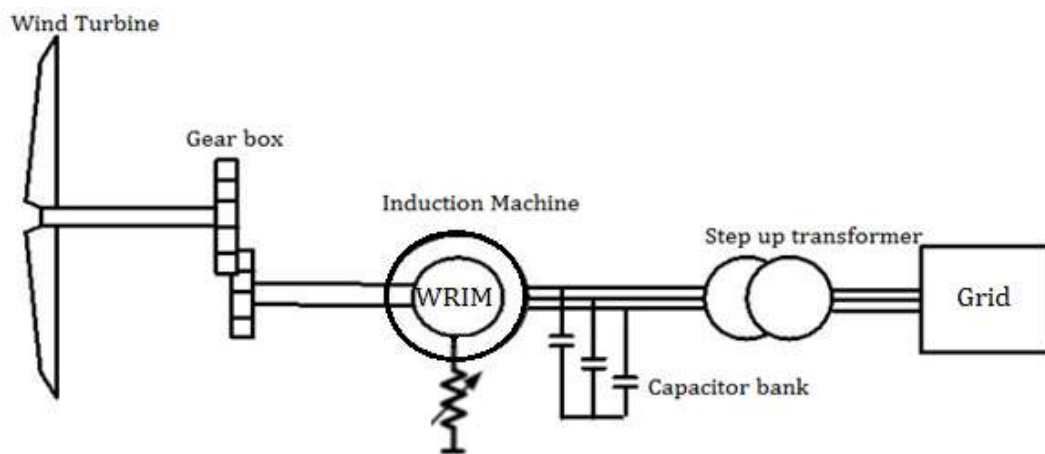


Figure 1.14: Schematic Circuit Diagram of Type 2 Wind Turbine Generator

### 1.4.3 Type 3 WTG

In Type 2 wind turbines, energy is dissipated in the rotor circuit resistors in order to operate it in the desired wind speed condition. To increase the energy efficiency, Type 3 wind turbine generators employ doubly fed induction generators. A doubly fed induction generator operates in a generalized fashion similar to synchronous machine. In synchronous generator the rotor is excited with DC current and the rotor is turned at synchronous speed. An AC voltage at a frequency corresponding to synchronous rotor speed is induced in the stator. In a doubly fed induction machine, the rotor is not restricted to run at synchronous speed. The difference between operating speed and synchronous speed for the stator frequency is

referred as slip speed, to keep the frequency in the stator corresponding to synchronous speed; the rotor is excited with AC current at the frequency corresponding to slip speed. The alternating excitation generates a flux in the air gap moving with slip speed and when the rotational speed of the rotor is added to it, the effective flux in the air gap spins with synchronous speed, thereby inducing voltage at a frequency corresponding to synchronous speed. The variable frequency AC excitation to rotor is commonly provided by means of an active converter and connected to the rotor circuit through brushes and slip rings.

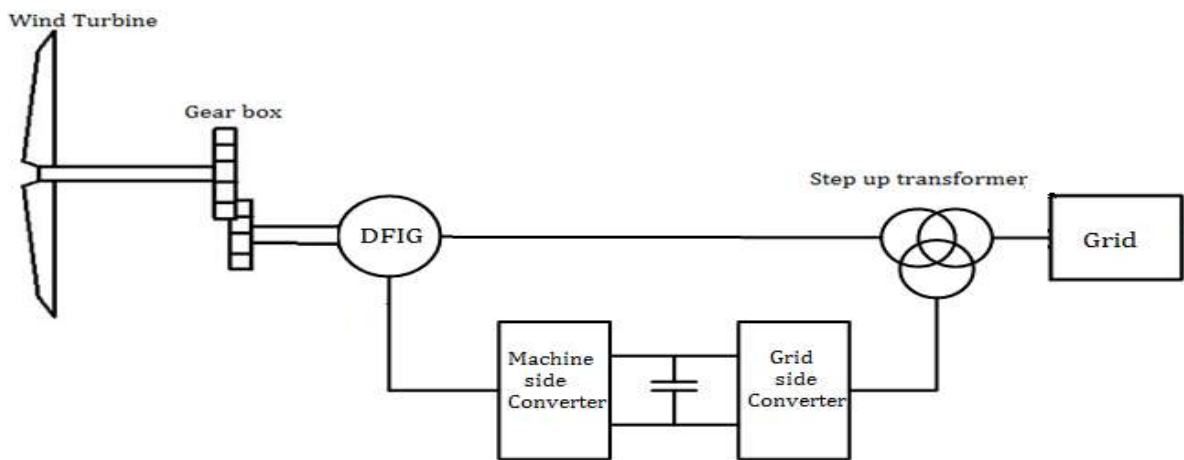


Figure 1.15: Schematic Circuit diagram of Type 3 wind turbine generation

The grid side converter in Figure 1.15 supplies power to the machine side converter when the rotor is operated below optimal speed and pushes power to grid when rotor is operating at super synchronous speed. There is no requirement for capacitor banks in Type 3 wind turbine generators, as the reactive power required by the machine is provided by changing the phase between current and voltage by means of a PWM controlled machine side converter. If the speed of the rotor becomes more than synchronous speed, the rotor is excited at a frequency corresponding to negative

slip speed i.e., changing the phase sequence of the rotor input from ABC to ACB. This way the effective speed of air gap flux is maintained at synchronous speed. There is an additional advantage by exciting the rotor with ACB phase sequence. In such a condition the converter provides negative power to the machine through the rotor circuit i.e., pulling out energy from the rotor.

#### **1.4.4 Type 4 WTG**

One of the main reasons behind the development of Type 4 wind turbine generators was the desire to install wind turbines off-shore where access for maintenance would be problematic. Doubly fed induction generators require maintenance in the rotor circuit as the carbon brushes wear; gearbox and transmission maintenance is also a huge factor. Type 4 WTGs don't need to have variable speed transmissions (or at least not mechanical transmissions). Type 4 wind turbines use machines that do not require control of rotor current. Instead the frequency of the rotor is allowed to vary with the wind speed.

Type 4 wind turbines commonly employ two types of machines, Permanent Magnet Synchronous Machines (PMSM) or Squirrel Cage Induction Machines (SCIM).

##### **1.4.4a Permanent Magnet Synchronous Machine - Operation**

Faraday's law of electromagnetic induction states that if a coil is placed in a varying magnetic field, a voltage is induced in the coil which is proportional to the rate of change of flux and number of turns in the coil. By Lenz's law, when an emf is generated by a change in magnetic flux according to the Faraday's law, the polarity of

the induced voltage is such that it produces a current whose magnetic field opposes the change that produces it. The value of the induced emf will be

$$\mathcal{E} = -N_t \frac{d\phi}{dt} \quad (1.13)$$

where:  $\mathcal{E}$  – Induced Electro Motive Force (EMF)

$N_t$  – Number of turns in the coil

$\phi$  - Flux

If the flux varies sinusoidally, the induced emf will also be sinusoidal. Generally the flux provided by permanent magnets is constant. If these magnets are mounted on the rotor shaft, the conductors in the stator circuit experience sinusoidally varying flux linkages as the rotor spins. As the rotor starts operation, each pole of the magnet moves in a circular fashion, thereby inducing a sinusoidal emf in the stationary stator coils as shown in Figure 1.16.

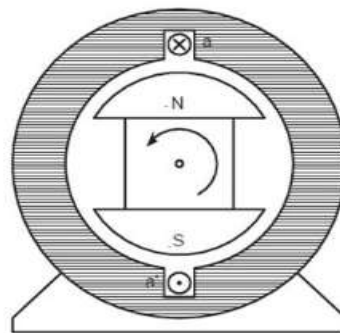


Figure 1.16: Permanent Magnet Synchronous Machine

The rotor flux required by the machine is provided by the permanent magnets, so there is no need to provide excitation externally. The torque responsible for turning the shaft is provided by the turbine. The frequency of voltage and current generated,

and the magnitudes of the current vary according to the wind speed. The turbine maintains a fixed gear ratio, there is no mechanical transmission. To synchronize the generator output with the grid a back-to-back ac/dc/ac converter is used as shown in Figure 1.17. The role of machine side converter is to rectify ac to dc. A simple diode bridge rectifier would serve the purpose, since the permanent magnet rotor does not require an external voltage source. The voltage is then converted to ac in synchronism with the grid by controlling the firing of the grid side converter. To provide the most flexibility for operation, the grid side converter is usually a voltage source converter. The output from GSC is synchronized by tracking the grid frequency using a Phase Locked Loop (PLL).

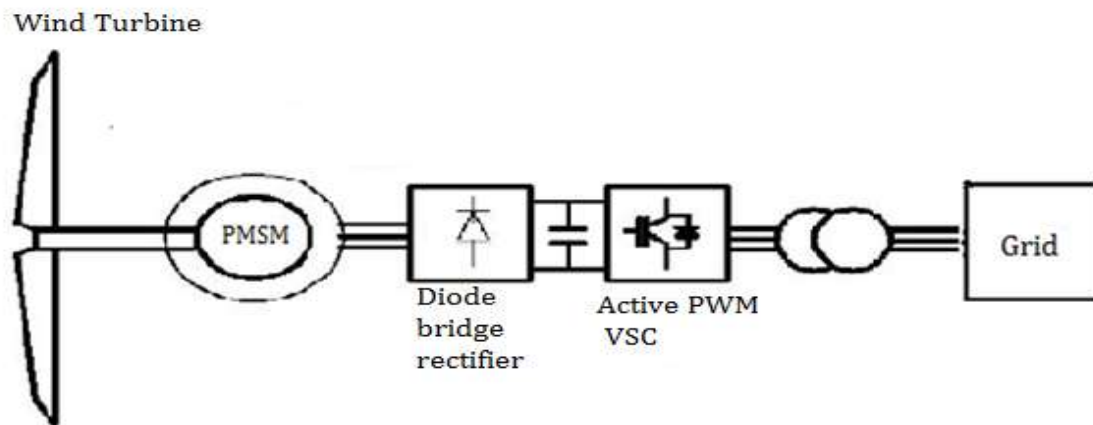


Figure 1.17: Schematic circuit diagram of Type 4 PMSM wind turbine generator

#### 1.4.4b Squirrel Cage Induction Machine - Operation

When a Type 4 WTG is implemented using a squirrel cage induction machine, the reactive power required for the air gap flux is provided through the stator winding by an active machine side converter as shown in Figure 1.18. The converter firing is

controlled in such a way that reactive power ( $Q$ ) is supplied to the machine and real power ( $P$ ) is extracted from the machine as would be the case for a regenerative induction motor drive. This control of real and reactive power will be explained in Chapter 3.

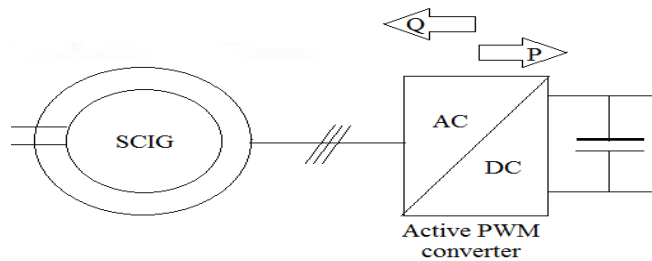


Figure 1.18: Squirrel cage induction machine and converter structure in Type 4 WTG

There is renewed interest in Type 4 wind turbines using squirrel cage induction machines due to a global shortage of rare earth elements required for manufacture of permanent magnets.

### 1.5 Need for protection of WTGs

Type 4 wind turbines, due to the controllability of the voltage source converters, can handle the fault current to a certain extent, but will eventually need to be disconnected from the faulted system for longer duration fault conditions or if voltage gets too low. Failing to do so might cause permanent damage to the wind turbines. If there are voltage sags in a WT integrated system due to power imbalances, disconnecting the WTG instantaneously could result in a worse condition. There are certain conditions that the WTG is expected to operate which are explained in Chapter 2.

Therefore it is essential to provide a protection scheme to operate within the normal operating conditions of wind turbines and react correctly to the faults.

Conventional protection schemes are failing to detect some types of faults for systems fed by Type 4 WTGs. A brief description of protection issues is given in Chapter 6 of this thesis. The objective of this thesis is to explore different operating conditions and design a protection scheme that operates accurately for the majority of fault situations.

### **1.6 What sets this research apart?**

With the increase in grid integration of Type 4 WTGs, it has become important to provide a scheme for protection. In [9] the author explained failures of conventional relays in providing the protection for Type 4 wind turbines, mentioning the different aspects of those protection schemes that had difficulty. In [11] the author addressed challenges that are being faced in association to the Type 4 wind turbine generators from the industrial point of view. The converter controller details are proprietary to the manufacturers and are not shared. In [15] the author described the fault current contributions by Type 4 WTGs during faults, providing evidence of failures of conventional protection schemes.

This research explores converter controller operation and designs a protection scheme addressing the situations and conditions where the conventional relays misoperate. The new scheme is simulated and tested in a real time digital simulator and validated by analyzing the responses to faults.

### **1.7 Overview of the Thesis**

The scope of this thesis is as follows,

1. Introduction to wind energy systems, listing of the objective of the thesis and description of the types of wind turbines with their operating principles.

2. There are grid codes that renewable generation such as WTs and PVs are expected to meet when interconnected to a power system. Chapter 2 explains grid codes imposed on WTs and PVs.
3. The modeling of a Type 4 wind turbine, control aspects of inner and outer control loops, compensator gain calculation and implementation in the simulation tool are presented in Chapter 3.
4. The model built has to be tested before going into protection analysis to ensure that the model provides the behavior similar to actual WTGs. This is presented in Chapter 4 with a description of the expected results, which are compared with the simulation responses.
5. Fault analysis with Type 4 WTs presented in Chapter 5, making note of differences in voltage and current waveforms for different types of faults from those seen with conventional synchronous generators.
6. The reasons why conventional relays can misoperate when faults are fed by Type 4 WTGs are explained in Chapter 6 in context of relay operating principles.
7. The new protection scheme designed for the protection of systems fed by Type 4 wind turbines is presented in Chapter 7, and validated with simulation.
8. Summary of the thesis is presented in Chapter 8 along with conclusions and suggestions for future work.
9. The test system parameters are presented in Appendix A.

## **1.8 Summary**

The basics of wind turbine operation and the types of wind turbines were discussed in this chapter. Methods to supply energy required to excite the machine were described

in general terms. The operating characteristics of the wind turbines were also described.

## Chapter 2 – Grid Codes

Transmission regulatory organizations have requirements that are designed to regulate the wind farms connected online to the grid system to improve response during large disturbances. These codes vary in scope and specific details from one jurisdiction to another. All transmission regulatory bodies have almost similar general goals; and have developed these specifications according to their specific type of operating conditions. References [2] and [5] described these codes effectively. The codes that apply to western part of the North American grid are described below. These apply for all generation, including wind turbines.

### 2.1 The typical requirements for grid connection

- *Voltage operating range:* There is certain standard voltage range that the power system operates over. This specific range could vary from system to system. In the Western part of North America this range is from 0.95 to 1.05 pu [22]. Wind turbines or any other generators are expected to operate in this typical operating range in synchronism to the grid.
- *Frequency operating range:* The power frequency of the grid varies within a certain range, which also varies from system to system. In the western interconnection generation is required to stay synchronized between 59.5 Hz and 60.5 Hz [22]. The wind turbines are expected to stay synchronized over grid frequency variations within this range.
- *Power control:* The wind farms are expected to have control over their real power output. Maximum ramp rates are also imposed on the generation

including wind turbine. The codes require ramping up or down capability from 0 to  $P_{max}$ , or from  $P_{max}$  to 0 within an adjustable interval. Generally meters are only for real power and hence there won't be any income for providing reactive power so most wind farm owners choose to normally operate at unity (1.0) power factor. But there are certain situations where they choose to provide reactive power for voltage stability reasons.

- *High voltage operation:* This is for the condition of voltage exceeding the operating range during a disturbance. Most grid codes require that wind turbines be capable of staying connected to the grid under temporary overvoltage conditions for a certain time as shown in Figure 2.1. For example, for the case in Figure 2.1, if the voltage reaches 1.4 pu due to some condition, the generator is expected to withstand this condition without disconnecting from the grid for a minimum of 2 cycles of operation i.e., 33ms.
- *Low voltage operation:* If a large imbalance between demand and supply arises due to sudden change in load or a fault occurs, the voltage of the system falls. If generators disconnect due to under voltage, the system has a power deficit after the fault is cleared, and the system becomes unstable. For this reason generators including wind farms are expected to stay connected to the grid for a set amount of time to allow the system to react and get back to normal condition. This time is dependent on the drop in voltage. The typical low voltage ride through requirement is shown graphically in Figure 2.1. The region that is not shaded is the region where the wind farms are expected not to trip. To aid this, many turbine designs require that the wind farm supply reactive power to reduce the

local voltage sag. Some jurisdictions give the grid operator control of capacitor banks, and they may stay connected if the generators trip.

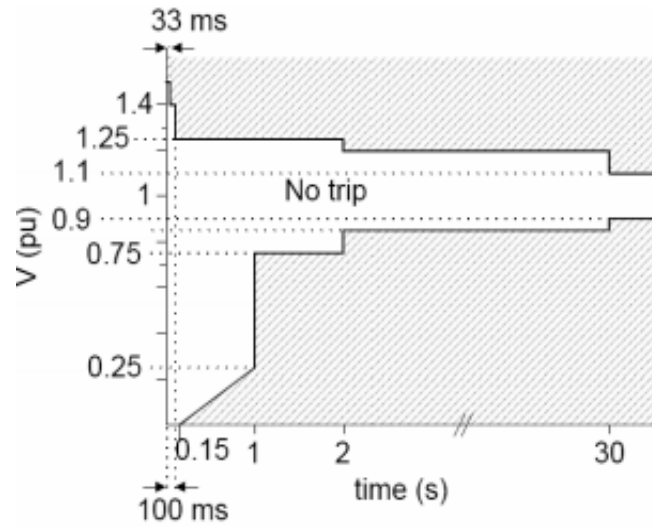


Figure 2.1: Typical grid voltage magnitude requirements [2]

## **Chapter 3 – Modeling of Type 4 WTG**

### **3.1 Objective**

The main objectives of this work are (1) designing a system to simulate the response of Type 4 WTGs to different types of grid side disturbances and (2) developing a new protection algorithm. The modeling is done keeping all aspects of the control architecture, including a realistic implementation of Pulse Width Modulation (PWM) switching.

### **3.2 Simulation Software- RSCAD/RTDS**

All the simulations involved in this research are performed using a Real Time Digital simulator (RTDS) with the RSCAD graphical interface software. RTDS allows the user to run simulations and get the outputs which can be interfaced to physical control hardware in real time in a closed loop fashion. The power circuit and control models are created using a graphical user interface. Simulations run continuously in real time and disturbances can be applied. Selected outputs can be interfaced to external hardware and the response of that hardware is fed back to the simulation.

### **3.3 Wind Turbine Power Circuit Model**

The system modeled is a Type 4 wind turbine generator with a permanent magnet synchronous machine. A simple diode bridge rectifier on the machine side serves the purpose of rectifying the machine output. As discussed earlier, there is no need to supply reactive power to the machine for establishing the flux in the air gap; the permanent magnet provides the required flux. The simulation model of the diode bridge rectifier is shown in Figure 3.1

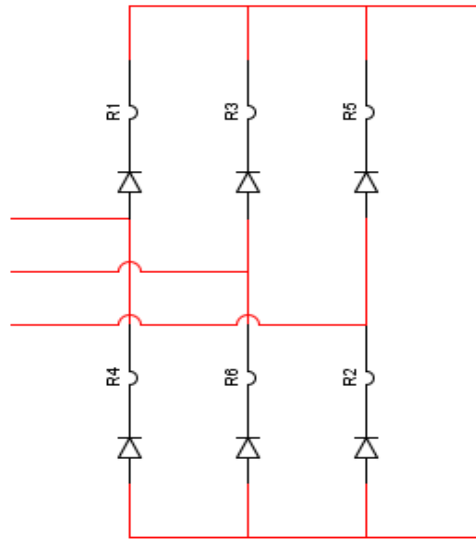


Figure 3.1: Diode bridge rectifier – simulation model

An active grid side voltage source converter is used to invert DC back to AC in synchronism with the grid.

The voltage source converters considered here are classified into two basic types based on number of switching levels of operation.

- Two level
- Three level

A two level three phase converter consists of 6 IGBT switches in a bridge configuration as shown in Figure 3.2. The firing is controlled to synthesize the output from the converter. There will be only two levels in ac line to line voltage  $+V_{dc}/2$  and  $-V_{dc}/2$ . The only control parameter are the on and off time of the switches.

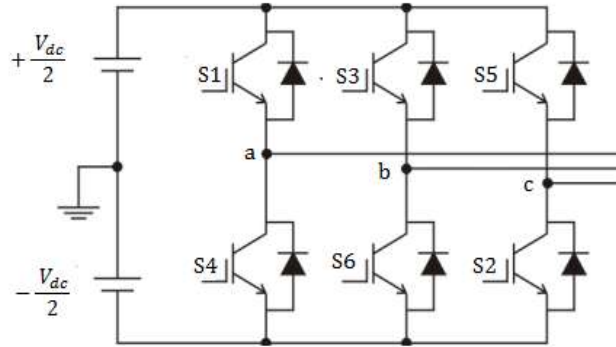


Figure 3.2: 2 Level Voltage Source Converter

The phase to phase outputs of the converter will look like the waveform in the Figure 3.3. The sinusoidal is fundamental 60Hz component of the output.

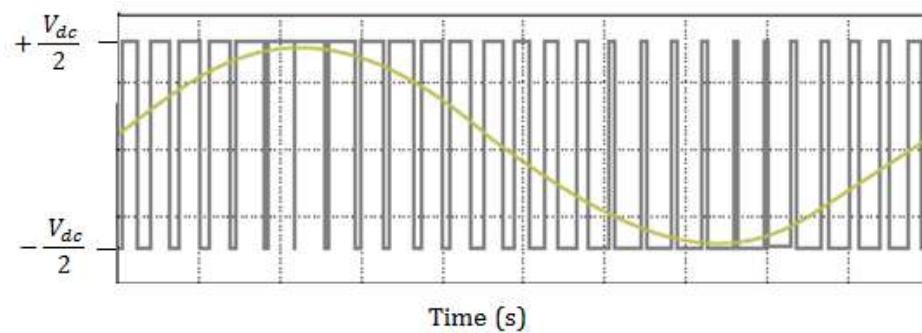


Figure 3.3: Output of two level converter – phase to phase voltage

It is evident from Figure 3.3 that there are only two levels of operation and the only parameter that can be varied to control the output are the on and off time of the switches. A three level converter operates at three ac voltage levels;  $+V_{dc}/2$ ,  $-V_{dc}/2$  and 0 and require a different control topology. Therefore there are two parameters that can be varied to control the output of the converter; on-off time of the switches, and the selection of the voltage level. The effective harmonic content and effective switching frequency content of a three level converter switching at 2 kHz is same as that of a two level converter switching at 4 kHz.

The actual switching frequency of a three level converter is less than that for a two level and hence the switching losses associated with those are also lower than for a two level converter. Losses are also reduced because  $\Delta V$  across switches is less at each switching due to multiple levels. For these reasons many manufacturers use three level converters for Type 4 WTG and photovoltaics (PV).

Three level converters can also be classified based on the switch topology. The most commonly applied types are shown in Figures 3.4 and 3.5:

- T type converter

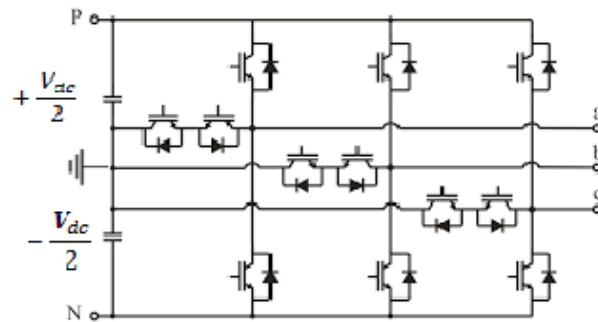


Figure 3.4: T type, 3 level converter

- Neutral point clamped (NPC) converter

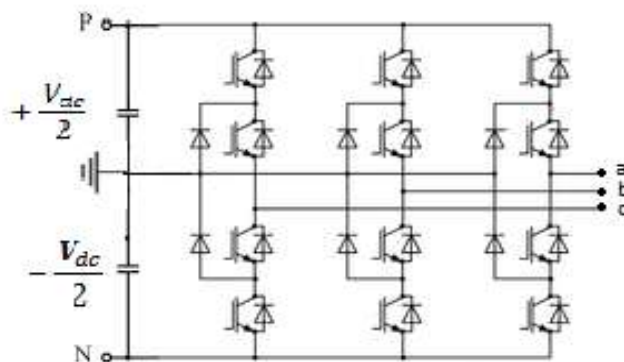


Figure 3.5: NPC type, 3 level converter

Both topologies can be extended to a larger number of levels. But three level converters are common in Type 4 WTG. The required voltage rating of the switches in bridges in a T type converter is higher than for a NPC type converter, and most manufactures are inclined to use NPC converters.

The neutral point of the converter in the DC link has to grounded. Failing to do so will create a floating neutral in the system. The output of a three level converter will look similar to Figure 3.6. It is visible that the output is controlled by varying the on-off time of the switch and the operating voltage level of the converter. The sine wave represents the fundamental 60Hz quantity of the output phase to phase voltage,

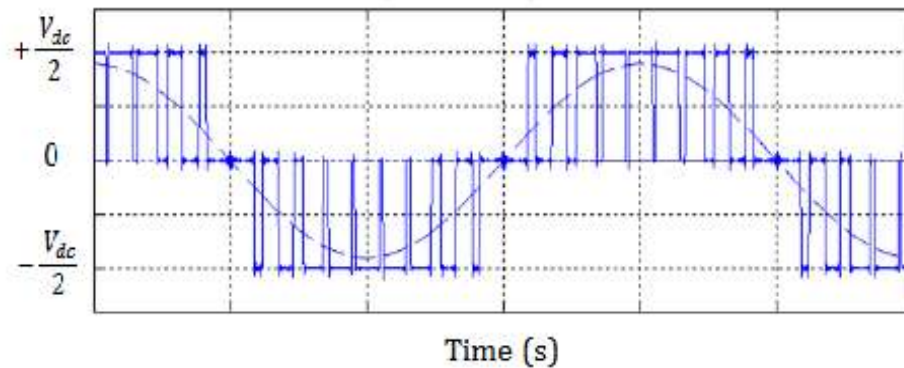


Figure 3.6: Phase to phase output of a 3 level converter

A three phase, three level NPC converter model is developed and used in this thesis. Figure 3.7 shows the RSCAD circuit schematic. The IGBT switches are modeled as ideal GTOs with a RLC numerical damping factor for IGBT switches due to unavailability of IGBT switch models. The resistance in the DC link is the capacitor internal resistance.

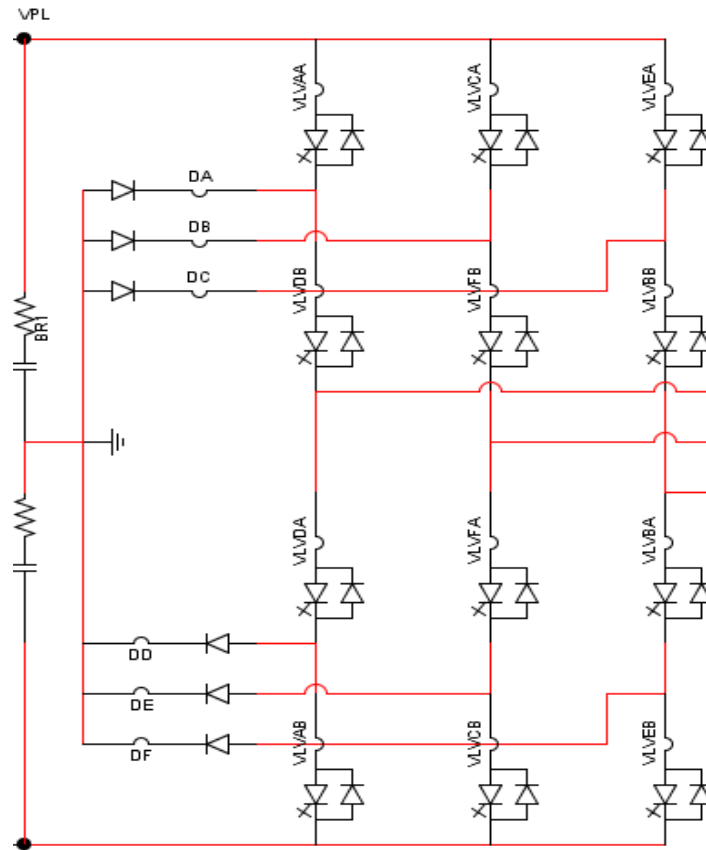


Figure 3.7: Simulation Model – Three phase, three level NPC converter

The firing pulses are generated by sine triangle pulse width modulation. The firing pulses for switches of each leg are obtained by comparing the modulating function for each phase to a unipolar triangular carrier signal (unlike the pulse width modulator for a two level converter which uses bipolar triangular carrier wave). The modulating wave for each phase is generated by a controller.

Considering 'A' phase leg of the 3 level NPC converter shown in Figure 3.8, the switching functions of the switches are obtained by comparing the modulating function  $m_a$  with a unipolar triangular carrier signal as shown in Figure 3.9.

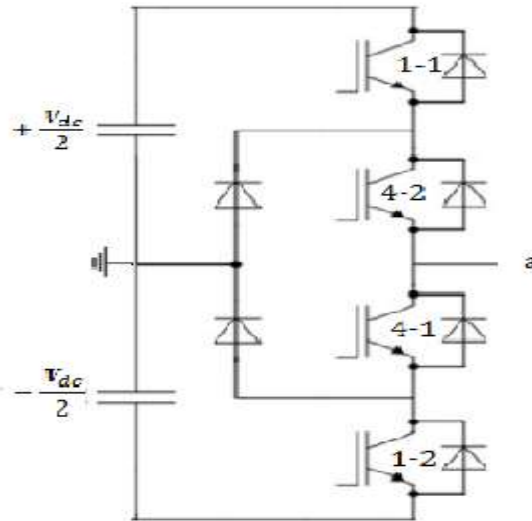


Figure 3.8: 'A' phase leg of a 3 level NPC converter

The switching functions are generating in such a way that the switches 1-1 and 4-1 are never on together, as is the case with 1-2 and 4-2. If such a condition occurs, the DC link might get shorted, damaging the switches. The modulating functions for 1-1 and 1-2 are  $m_a$  and  $-m_a$  respectively, and the switches 4-1 and 4-2 are operated in compliment to 1-1 and 1-2 respectively. The schematic representation of this control is shown in Figure 3.10.

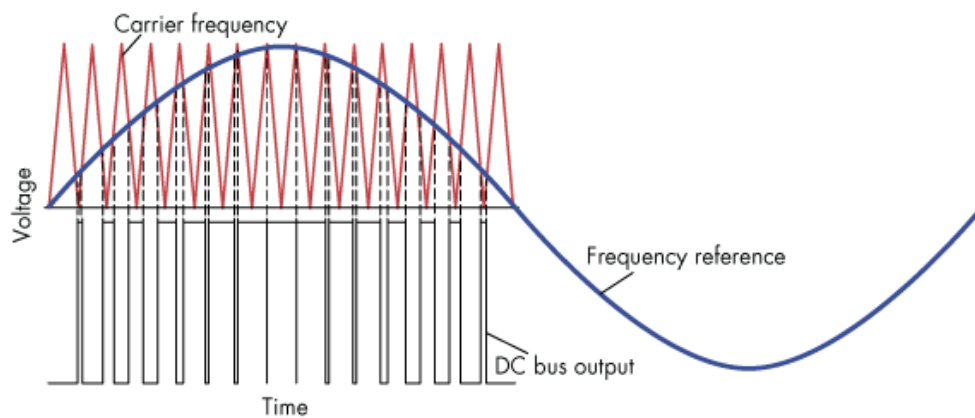


Figure 3.9: Schematic diagram of sine triangle PWM with unipolar triangular wave

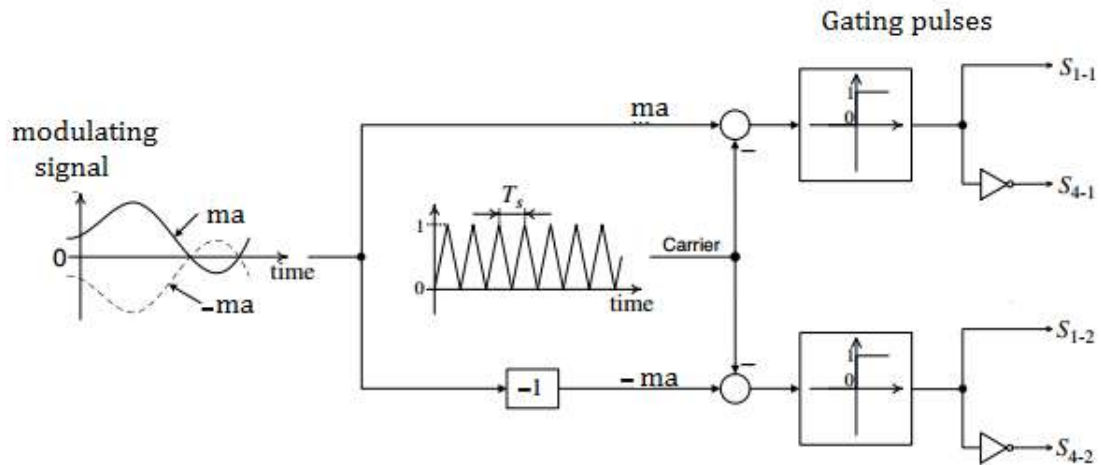


Figure 3.10: Schematic diagram of a PWM scheme for 3 level NPC converter [1]

The gating functions for other two phases are generated in a similar fashion. The switching frequency for this project is 2.04 kHz. The output from the power electronic converter contains harmonics along with the fundamental quantity. Under balanced steady state operation only odd harmonics of the switching frequency are produced. To filter out the voltage harmonics, a low pass filter is used. The filters generally used are either an L filter or an LCL filter shown in Figure 3.11. The inductors in the filter are normally an air core reactor whose internal resistance cannot be neglected. The other side of the filter is connected to a delta-star grounded step up transformer whose primary is connected to the collector feeder. This point is termed as Point of Interconnect (POI) or Point of Common Coupling (PCC). The system up to the PCC is owned by the wind farm owner and the other side is owned by a transmission operator. It is the responsibility of the wind farm owner to provide appropriate protection relaying at the point of interconnection to protect for faults inside the wind farm. The

transmission operation is responsible for protecting the transmission line in most cases.

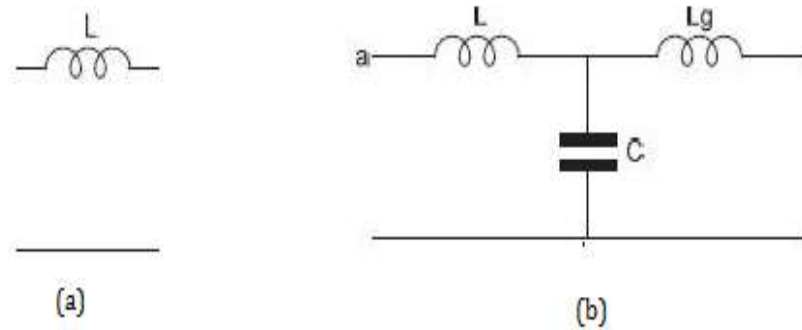


Figure 3.11: Circuit diagram of L and LCL filters

### 3.4 Controller Design and Control Aspects

The controller generates the modulating functions for the three phase legs based on real and reactive power set points. There are various factors that need to be considered in generating these modulating waves. The major factors are the phase voltage magnitude and frequency, at which the power needs to be exported, which is determined by measuring the voltage at the PCC. The frequency measurement is implemented using a phase locked loop in this case.

RSCAD has a built in phase locked loop model. When this block is fed with the 3 phase quantities, it tracks the frequency and phase of the input and outputs.

The control architecture is divided into two control loops, an outer control loop and an inner control loop. The outer control loop determines reference currents based on the required real and reactive power values and the inner control generates the modulating functions by comparing the reference current values with the actual

measured current values. The inner current control loops are implemented in synchronous DQ reference frame to decouple real and reactive power. The specific control loops will be discussed in Sections 3.6 and 3.7

### 3.5 Park's transformation

The instantaneous three phase quantities are time varying, which complicates fast closed loop design. The Park's transformation is a mathematical transformation that transforms three phase quantities to a two axis reference frame, here rotating at system frequency. The idea was initially proposed by R.H. Park for synchronous machines. The two axes are referred to as the direct (d) and quadrature (q) axes. The O is a common mode or zero sequence term. Balanced, steady-state operation will result in constant values for the d and q axis quantities in the synchronous reference frame. The O axis term will be zero

The dq0 transformation is described in the following discussion. Consider a set of balanced three phase AC quantities which are separated from each other by phase angle of 120 degrees. Equations (3.1), (3.2) and (3.3) show a three phase set of the equations when phase A is taken as reference.

$$f_a = |f_a| \cos(\omega t) \quad (3.1)$$

$$f_b = |f_b| \cos\left(\omega t - \frac{2\pi}{3}\right) \quad (3.2)$$

$$f_c = |f_c| \cos\left(\omega t + \frac{2\pi}{3}\right) \quad (3.3)$$

Where:  $|f_x|$  is the peak amplitude of the quantity

$\omega$  is the angular frequency  $2\pi f$

These quantities can be transformed into dq0 axis values  $f_d, f_q$  and  $f_0$  using the Park's transform matrix (3.4).

$$\begin{bmatrix} f_d \\ f_q \\ f_0 \end{bmatrix} = \sqrt{\frac{2}{3}} \begin{bmatrix} \cos(\theta) & \cos\left(\theta - \frac{2\pi}{3}\right) & \cos\left(\theta + \frac{2\pi}{3}\right) \\ \sin(\theta) & \sin\left(\theta - \frac{2\pi}{3}\right) & \sin\left(\theta + \frac{2\pi}{3}\right) \\ \frac{1}{\sqrt{2}} & \frac{1}{\sqrt{2}} & \frac{1}{\sqrt{2}} \end{bmatrix} \cdot \begin{bmatrix} f_a \\ f_b \\ f_c \end{bmatrix} \quad (3.4)$$

The value  $\theta$  is the angle of the reference frame. It can be 0 for stationary frame or  $\omega t$  for a rotating reference frame. The vector representation is shown in Figure 3.12, where  $f_d, f_q$  are space vectors for stationary frame.

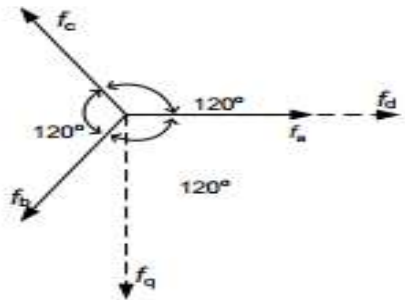


Figure 3.12: dq0 transformation of 3 phase quantities

The simplified time domain equivalent representation of transformation to the synchronous reference frame can be explained as follows. The 0 axis value is non zero only when there is a ground imbalance in a three phase set. Since we are considering a set of balanced three phases, it is zero. The d (direct) axis value is obtained by sampling the reference phase quantity at its own frequency. The q (quadrature) axis value is sampled at the same frequency, but with a 90 deg phase difference with respect to the direct axis quantity. If the sampling frequency is synchronized with the signal frequency,  $f_a$  is sampled at the point on wave in each cycle, generating constant values.

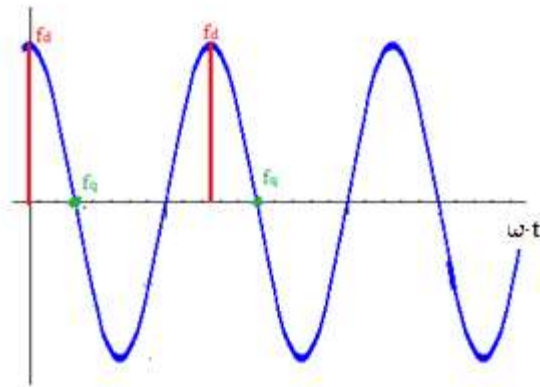


Figure 3.13: Time domain representation of dq0 transformation

The complex 3 phase power in terms of voltage and current phasors is given by:

$$P_{3\phi} - j \cdot Q_{3\phi} = V_a \cdot I_a^* + V_b \cdot I_b^* + V_c \cdot I_c^* \quad (3.5)$$

$$P_{3\phi} - j \cdot Q_{3\phi} = [V_a \quad V_b \quad V_c] \cdot \begin{bmatrix} I_a \\ I_b \\ I_c \end{bmatrix}^* \quad (3.6)$$

When transformed into the dq0 reference frame equation (3.5) transforms into (3.7) and (3.8). Also when the 3 phase quantities are balanced, the zero axis quantities become zero. If the sampling reference is taken in such way that the voltage q axis sample value coincides with zero, then we get  $V_q = 0$  which further simplifies the equation.

$$P_{3\phi} = \frac{3}{2} [V_d \cdot I_d + V_q I_q + V_0 I_0] \quad (3.7)$$

$$Q_{3\phi} = \frac{3}{2} [-V_d \cdot I_q + V_q I_d + V_0 I_0] \quad (3.8)$$

Putting  $V_q = 0$  and ruling out the zero axis quantities for balanced three phase operation results in,

$$P_{3\phi} = \frac{3}{2}[V_d \cdot I_d] \quad (3.9)$$

$$Q_{3\phi} = \frac{3}{2}[-V_d \cdot I_q] \quad (3.10)$$

Using equations (3.9) and (3.10) in balanced steady state conditions, the real power and reactive power are directly dependent on the d axis and q axis current values respectively. Real and reactive power is regulated directly by controlling these values, making the control loop design simpler and easier. But, when the control is done in synchronous dq reference frame, the output modulating functions will also be in dq reference frame. Therefore the modulating functions need to be transformed back to ABC frame of reference in order to generate switching functions.

The RTDS blocks used in the model for transforming quantities from the ABC frame to the dq0 reference frame and vice versa are shown in Figure 3.14.

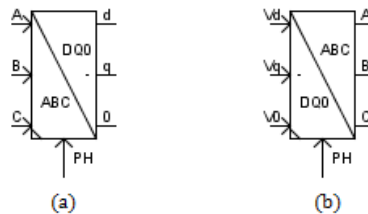


Figure 3.14: Simulation blocks (a) ABC – dq0, (b) dq0 - ABC

### 3.6 Outer Control Loop

A relatively slow outer control loop is created for determining  $I_d$  and  $I_q$  reference values from the set point values for real and reactive power. In the case of a wind turbine generator, the output power from the wind is hard to forecast accurately. The wind will also be continuously varying, so it is difficult to determine the  $I_d$  current

reference value directly. The inverted  $I_d$  reference value needs to follow the generator output, otherwise either energy gets dumped in the capacitor and the dc bus voltage level increases and could possibly damage the power electronic devices, or if the power input falls, and the inverter supplies more ac power than is coming into the DC link and the voltage will fall as the capacitors get drained and the system will not be able to maintain the voltage at the inverter terminals. This will also have effect on the machine terminals as they are connected to the DC link by a diode bridge rectifier.

Therefore to overcome this problem i.e., to vary the exported ac power with the change in input, the input to the power control loop is based on regulating the DC link voltage. The generic energy flow is shown in Figure 3.14. The control scheme is based on keeping the DC link voltage constant, which means keeping the energy stored in the DC link constant. This effectively means maintaining power balance between the generator and the inverter. If the wind input increases,  $P_{in}$  increases, while at that instant the  $P_{out}$  is constant; the excess energy gets stored in the capacitor. This additional energy increases the voltage level of the DC link. When the controller senses the increase in voltage level increases the  $I_d$  reference value to increase  $P_{out}$ . This control scheme is in common use in many applications with dc links.

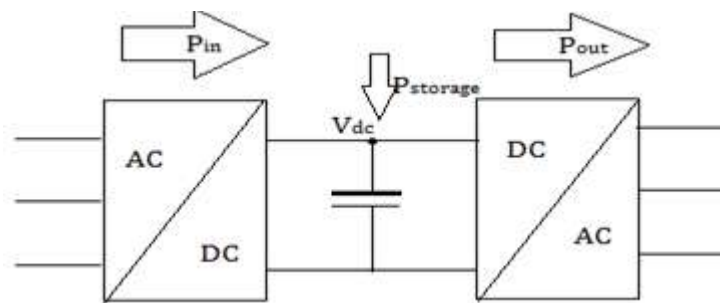


Figure 3.15: generic power flow diagram of AC/DC/AC converter.

When it comes to the reactive power control, it has already been stated that there is no compensation provided to the wind farm owner if they supply reactive power to the grid. Therefore the reactive power supplied to the grid is typically zero under normal steady state conditions. However the WTG designer may export reactive power under lower ac system voltage conditions. In order to meet LVRT codes, the converter supplies reactive power. Under normal operating conditions the reactive power supplied is zero which means the value of the  $I_q$  reference is zero.

Figure 3.16 shows a block diagram of the outer control loop for determining the  $I_d$  current reference. The per unit voltages across each capacitor in the DC link are taken and compared with the set point value. The error signal is passed to a PI compensator and the output obtained is checked against the operating limits. The final output is the  $I_d$  reference current.

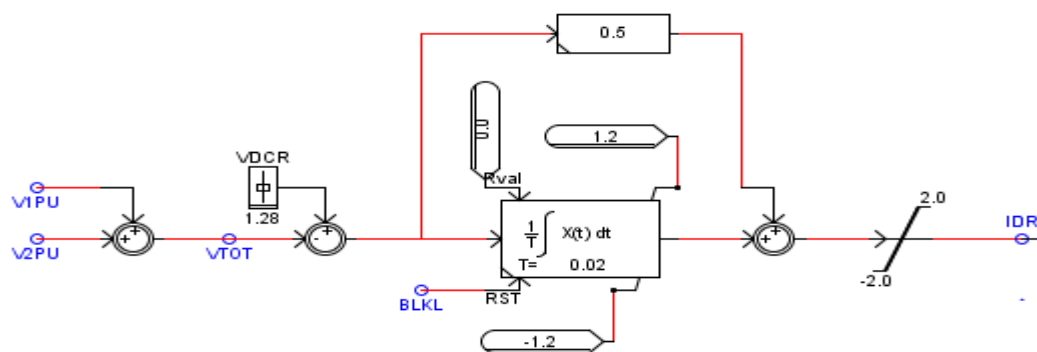


Figure 3.16: Control model of outer control loop

### 3.7 Inner Current Control Loop

The inner control loops generate modulating waves for all three phases for the use in switching functions. These modulating waves will be a scaled replica of the converter terminal voltages. The controller determines the voltage that has to be

supplied at the terminal to drive the current corresponding to the reference values. Since the control is done in dq frame the output values  $m_d$  and  $m_q$  are transformed back to ABC reference to get modulating waves  $m_a$ ,  $m_b$  and  $m_c$ .

A closed loop control is preferred due to the sensitivity of the output and to protect the power electronic devices from excessive currents. The  $I_d$  and  $I_q$  reference values are compared with the processed measured values. Different types of compensators may be used depending on the type of the reference signal and desired performance. The inner control loops are often implemented using proportional-integral (PI) compensators. The integral term of the compensator ensures that the reference values are closely tracked and guarantees zero steady-state error.

The controller gains can be determined by observing the plant loop. Consider the plant connection of one of the phases shown in Figure 3.16.

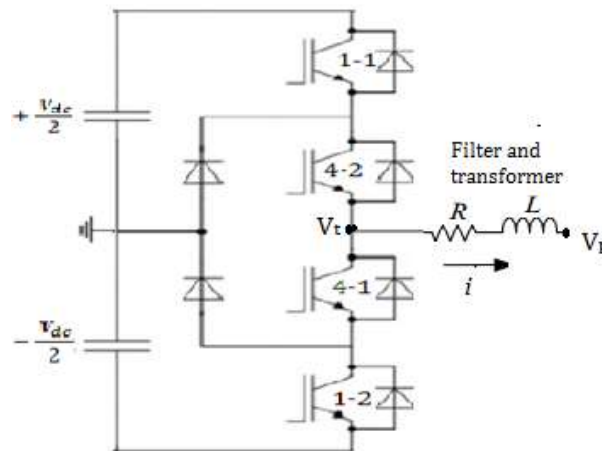


Figure 3.17: Phase 'A' Circuit representation of converter, filter and transformer

Let  $V_t$  be the line to neutral voltage at the inverter terminal and  $V_p$  be the voltage at the Point of Interconnect. These two points are connected by means of a filter, to reduce the

switching harmonics and a step up transformer. Let  $R$  and  $L$  be the resistance and inductance of the circuit. Let  $r_{on}$  be the on-state resistance of the switches. The voltage at the converter terminals is a function of modulating function for that phase and scaled by half of the DC Voltage.

$$V_t = m_a(t) \cdot \frac{V_{dc}}{2} \quad (3.11)$$

The Kirchoff's voltage loop equation, for the ac side of Figure 3.16 is:

$$V_t - V_p = (R + r_{on})i + L \frac{di}{dt} \quad (3.12)$$

The Laplace domain block diagram implementation of (3.12) is shown in Figure 3.18.

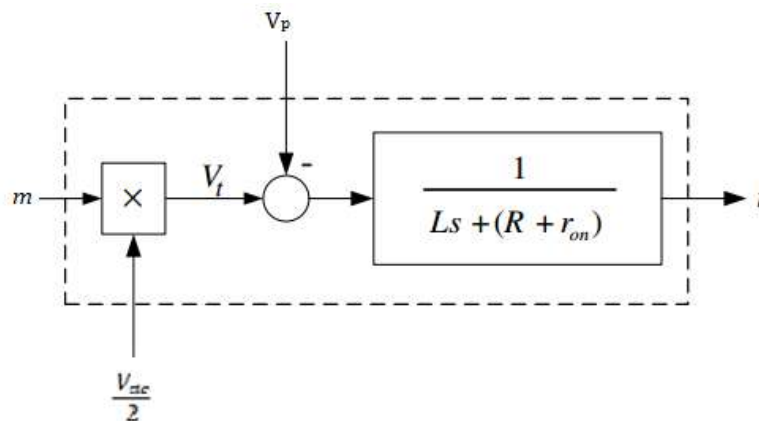


Figure 3.18: Control model of the loop equation [1]

In the inner current controller, the current reference command is compared with the measured values and an error signal  $e$  is generated. The compensator processes  $e$  and provides the control signal  $u$ . The control signal  $u$  is passed through a limiter prior to being delivered to converter pulse width modulation (PWM) signal generator. The control loop block diagram of the converter system is shown in Figure 3.19.

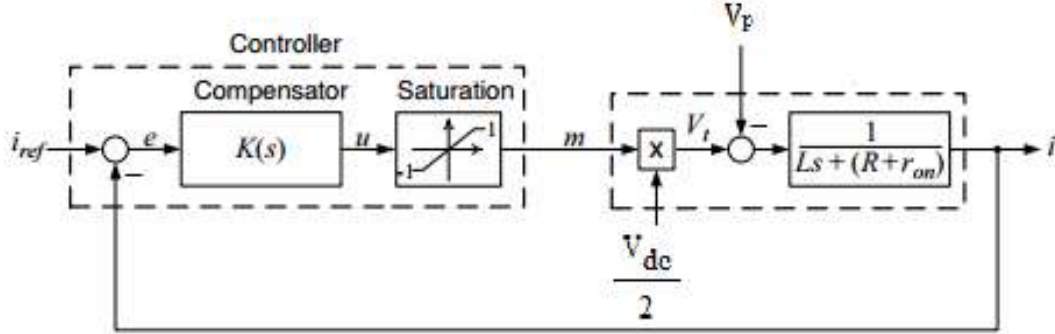


Figure 3.19: Control block diagram of the converter system

The loop gain of the above control system is:

$$l(s) = K(s) \frac{1}{Ls + (R + r_{on})} \quad (3.13)$$

Since the compensator is a PI controller, its transfer function will be of the form

$$K(s) = K_p + \frac{K_i}{s} \quad (3.14)$$

Substituting for the value of  $K(s)$  in equation (3.13) gives

$$l(s) = \left( K_p + \frac{K_i}{s} \right) \frac{1}{Ls + (R + r_{on})} \quad (3.15)$$

Rearranging the equation

$$l(s) = \left( \frac{K_p}{Ls} \right) \left( \frac{s + \frac{K_i}{K_p}}{s + \frac{R + r_{on}}{L}} \right) \quad (3.16)$$

Based on the loop gain, the system has a stable pole at  $p = -(R + r_{on})/L$ , close to the origin, corresponding to a slow natural response. If the pole of the system cancels the zero of the compensator, the open loop frequency response is improved. The time constant of

the controller is generally chosen as 5ms [1]. Applying this information leads to equations (3.17) and (3.18).

$$\frac{K_i}{K_p} = \frac{R+r_{on}}{L} \quad (3.17)$$

$$\frac{K_p}{L} = \frac{1}{\tau_i} \quad (3.18)$$

Where  $\tau_i$  is the deserved time constant of the controller, such that the controller reaches 63.2% of the steady state value in  $\tau_i$  seconds. Equations (3.17) and (3.18) can be solved to determine compensator gains  $K_i$  and  $K_p$ .

The control block model of the Id and Iq current regulator is shown in Figure 3.20. The measured values of current at the POI (IAP, IBP and ICP) are processed through a high pass filter to reduce the switching harmonics and are scaled to per unit. The resultant current is fed to an ABC-DQ0 transformation block. The block introduces a phase shift which is subsequently corrected. After the phase correction the actual values are compared with reference values, and the error signal generated is fed through a PI compensator. To improve response to large changes in operating points, the transformed voltages at the POI (Vd and Vq) are added in through a feed forward loop. As the control loop is in per unit the resultant outputs are the modulating waves in the synchronous DQ reference frame. These quantities are transformed back to the ABC reference frame using the DQ-ABC transformation block. The output ABC modulating waves are used for the generating the firing functions of the switches. The firing pulses for each simulation switch are generated separately with the functions generated by comparing the modulating wave with a unipolar triangular carrier signal.

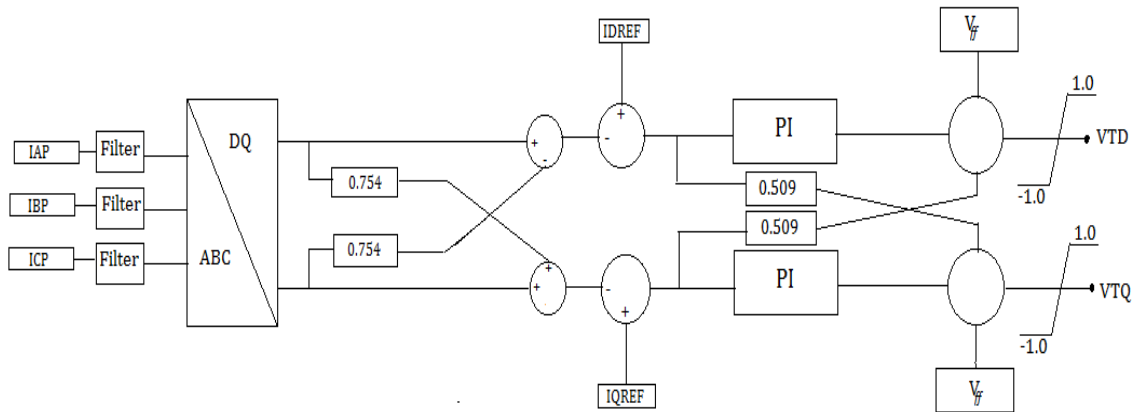


Figure 3.20: Simulation model - ID and IQ current regulator

Each block in Figure 3.20 is described in more detail in Appendix A

The schematic diagram of the system taken and modeled in this research is shown in Figure 3.21. The system parameters are also described in more detail in Appendix A.

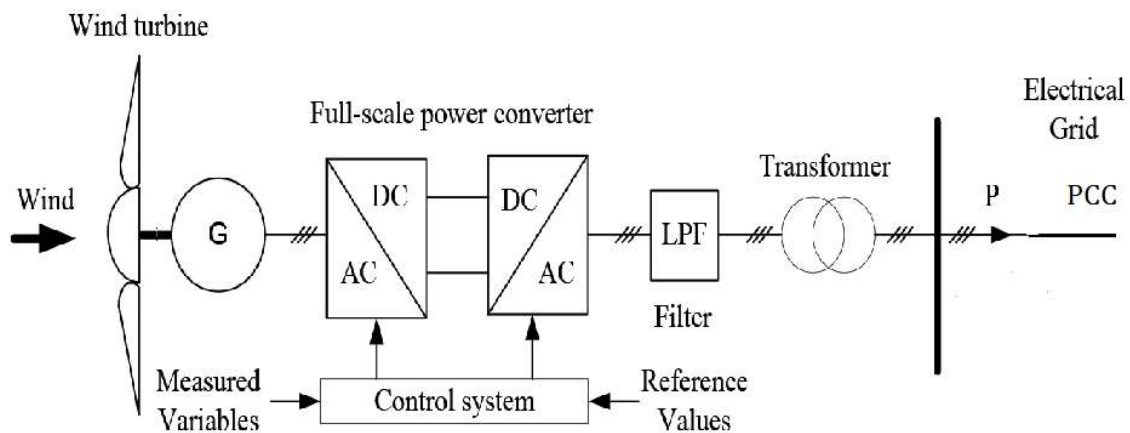


Figure 3.21: Test system diagram

The grid is modeled as a Thevenin equivalent source behind an impedance, and is connected in parallel with a resistive load which are connected through a transmission line.

### **3.8 Summary**

In this chapter, various design aspects of the Type 4 WTG system, including a typical controller design are discussed. The basic operational difference between 2 level converters and 3 level converters is explained. The compensator gains are also calculated based on the system parameters.

The model simulation results for validation are discussed in the next chapter.

## Chapter 4 – Converter Model Testing and Simulation Results for Normal Operation

### 4.1 Introduction

With the converter models completed in Chapter 3, the accuracy of the models needs to be established by testing the system under steady-state operation.

### 4.2 The voltage at the inverter terminals

The 3 level NPC converter is expected to have 3 levels in its operating voltage waveform. Figure 4.1 shows the voltage the terminal voltage from the inverter simulation. The left side shows a period of 10 cycles. The right side of the figure zooms in for one cycle. These waveforms match expectations.

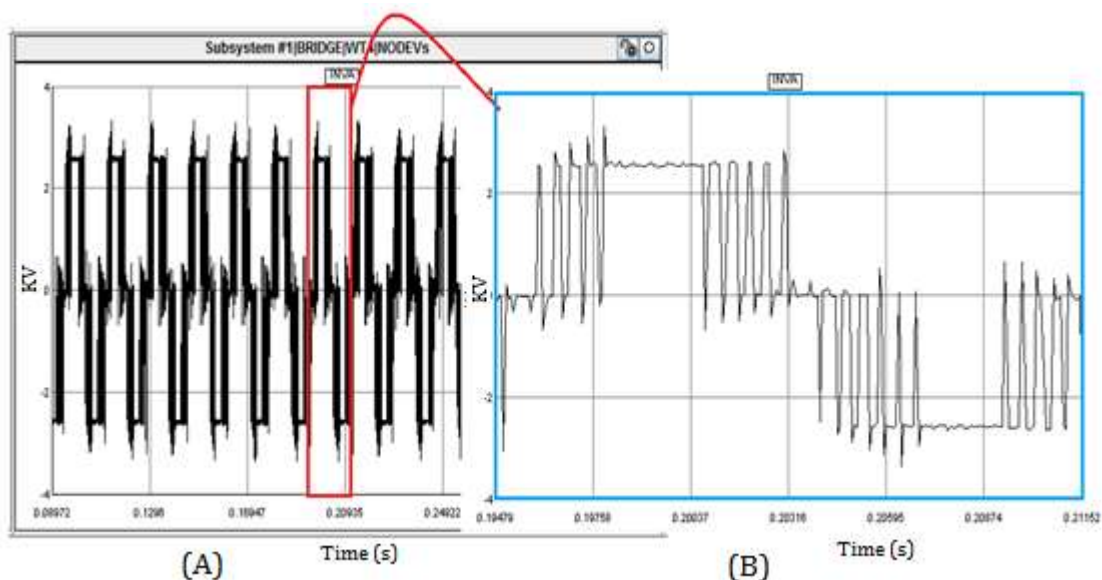


Figure 4.1: Terminal voltage of the inverter–A phase over(A)10 cycles and(B)1 cycle

### 4.3 Current Regulator Response

The  $I_d$ ,  $I_q$  reference values are compared with measured values in the controller. The reference value of the  $I_q$  current is set to zero. The measured values need to track the reference values.  $I_{DR}$  and  $I_{QREF}$  are the reference  $I_d$  and  $I_q$  values in Figure 4.2 and  $I_{GD}$  and  $I_{GQ}$  are the filtered outputs of the measured  $I_d$  and  $I_q$ . The simulation results comparing these values are shown in the following Figure 4.2. It is evident that the measured values are tracking the reference values. Since the time constant is 5ms, it takes 5ms to reach 63.2% of the steady state value for a change in reference values.

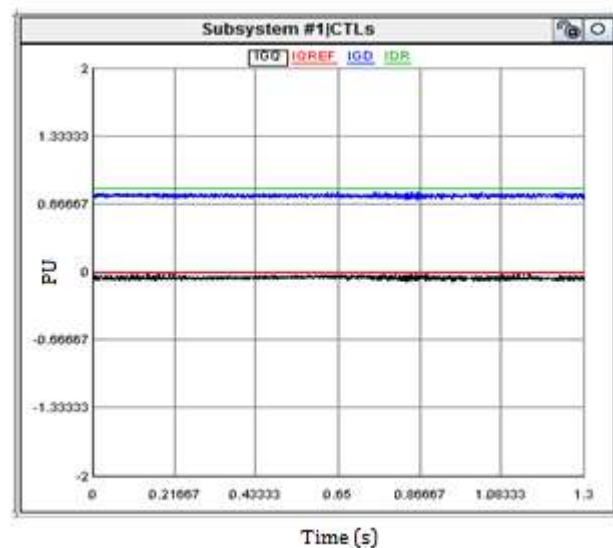


Figure 4.2: Id Iq reference and measured values

### 4.4 Voltages and Currents at Point of Interconnect

The voltage and currents at the Point of Interconnect represent the injection into the power system after the output filter. The voltage and currents at the POI have to meet grid codes with minimal harmonics. Figure 4.3 (A) and (B) show voltage and current waveforms respectively.

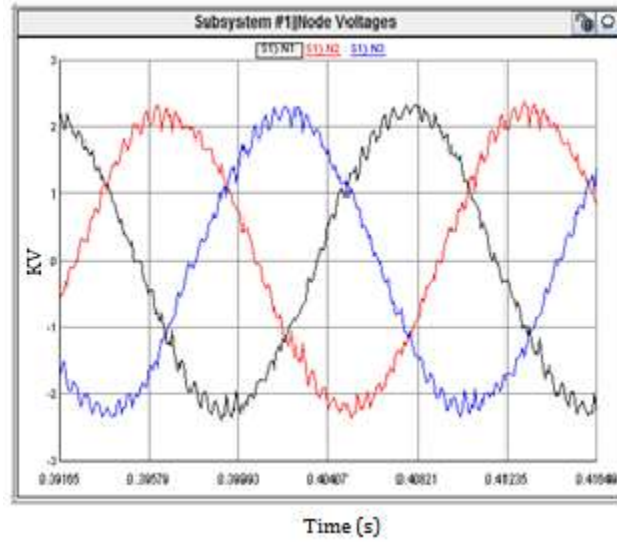


Figure 4.3A: Voltages at the Point of Interconnect

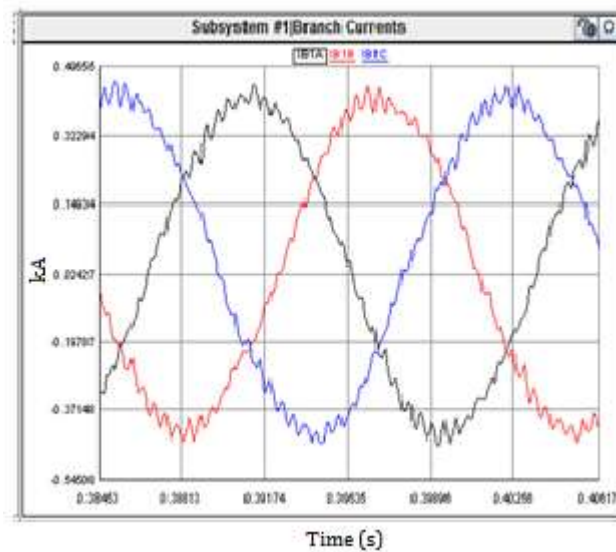


Figure 4.3B: Currents at the Point of Interconnect

#### 4.5 Voltages and currents at Machine terminals

Next the voltage and currents at the generator terminals are examined. Since the machine is a permanent magnet generator there won't be field control circuit. The terminal voltage will be sinusoidal under open circuit conditions. To understand

machine behavior when feeding a rectifier load, first considers a case of a single phase full wave rectifier with an AC source.

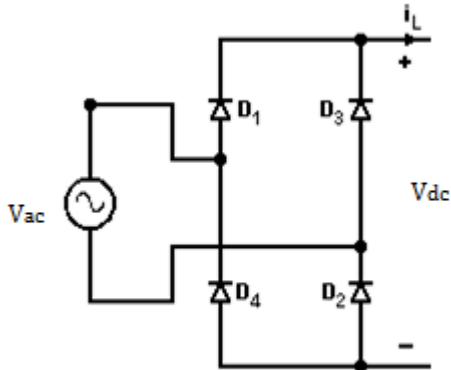


Figure 4.4: Single phase full wave rectifier

The terminal ac voltage will be purely sinusoidal and the rectified output voltage will have a DC offset with a ripple at twice the ac frequency as shown in Figure 4.5.

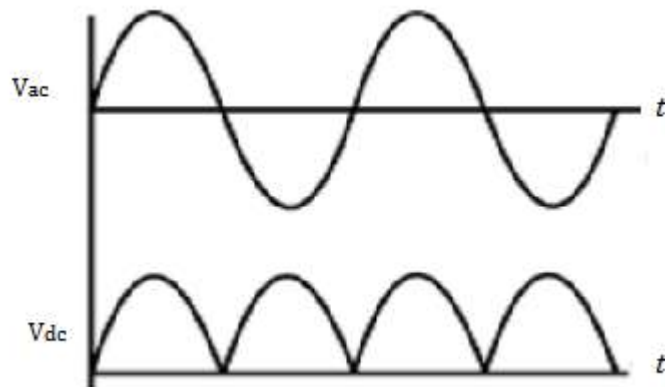


Figure 4.5: Input and output of a 1 $\phi$  full wave rectifier

But the DC side voltage shows a different type of characteristic when the rectifier output is connected to a capacitor with large capacitance. The capacitance stores charge on the DC side. This impacts the ac side current since current only flows when the ac

voltage exceeds the DC capacitor voltage. The DC side average voltage will be  $\frac{2}{\pi}V_m$ , where  $V_m$  is the peak amplitude of AC side voltage. The voltage waveforms on the rectifier input side and output side voltage when there is an infinite capacitance in the DC side are shown in the Figure 4.6. This response is because of the voltage drop across the ac source impedance of the current harmonics.

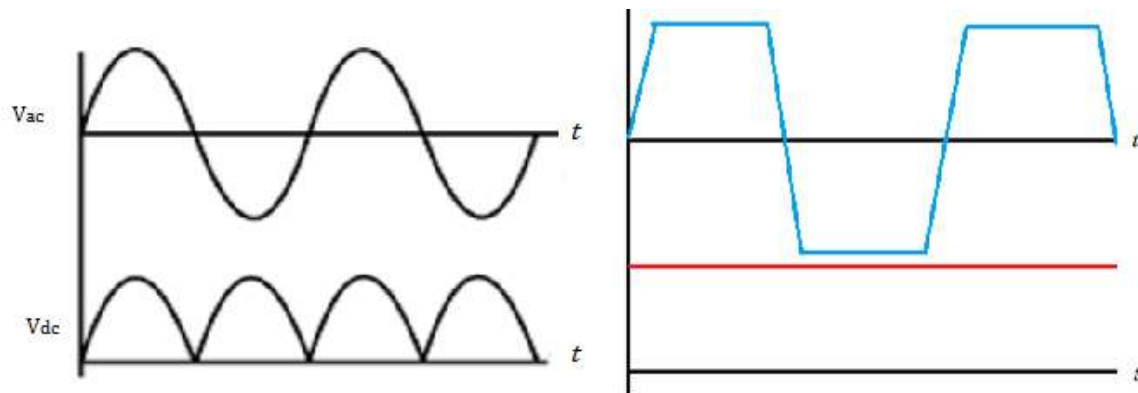


Figure 4.6: Comparison of In/Out of 1 $\phi$  full wave rectifier with capacitor on DC side

The 3 phase rectifier will exhibit the similar behavior. Figure 4.7 shows simulation results with the voltages at the machine terminals. To understand what is happening it is necessary to look at the currents.

There is only a limited time where the instantaneous source voltage will be more than the DC side voltage, and the current flows only in that particular part of the cycle. This can be observed in Figure 4.8.

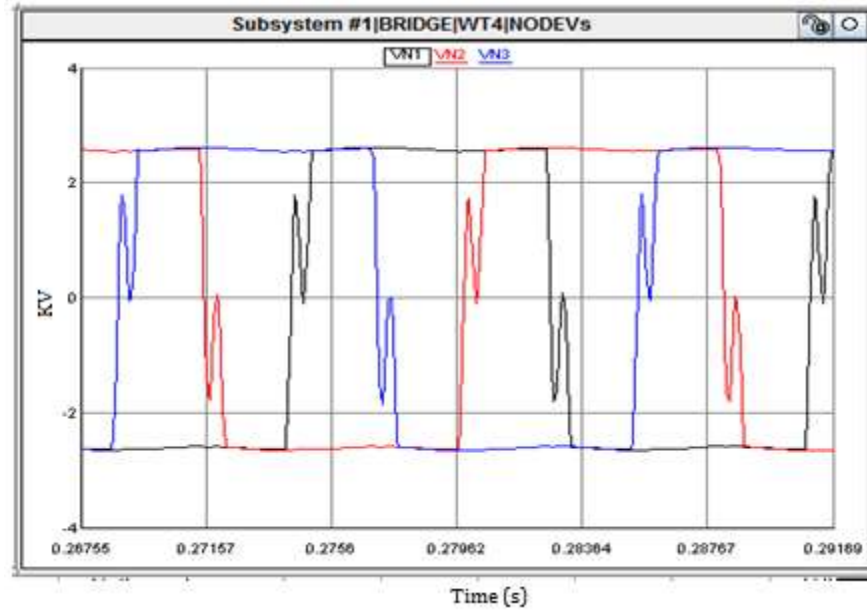


Figure 4.7: Voltage waveforms at the PMSM terminals

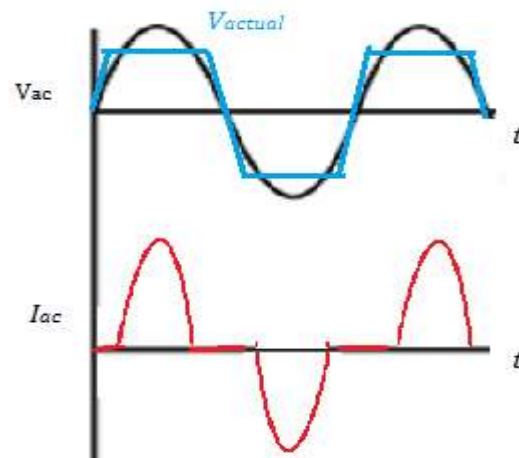


Figure 4.8: Current in the AC side for a 1 $\phi$  full wave rectifier

But for a 3 phase rectifier the ac current peaks occur two times in a half cycle, once when AB line-to-line voltage approaches to peak and once when AC line to line voltage reaches peak magnitude value. Therefore there will be two peaks in current in a half cycle. The simulation results are shown in Figure 4.9.

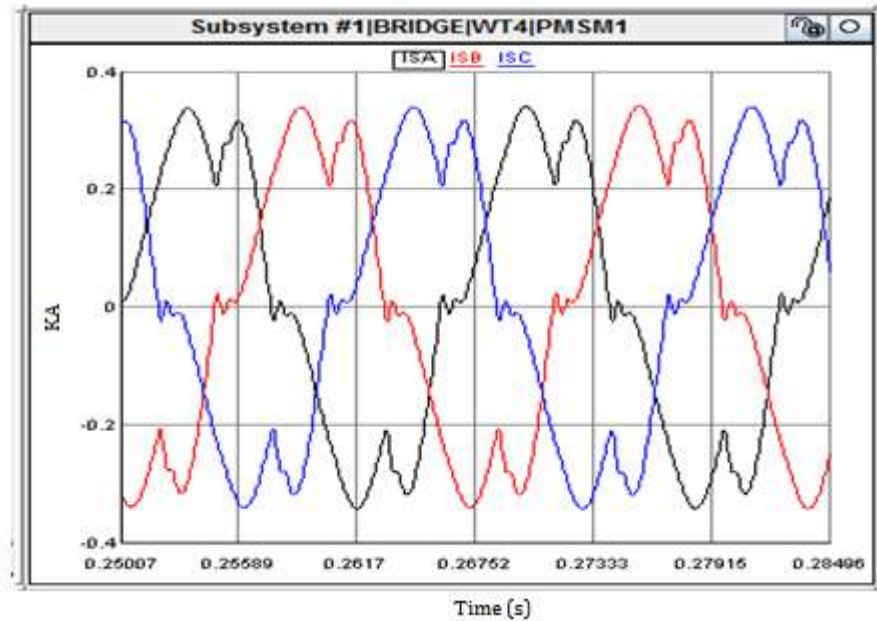


Figure 4.9: Currents at PMSM terminals

The machine terminal voltage is produced by the voltage drops of the current harmonics across the machine impedances.

#### 4.6 Summary

In this chapter, the model of Type 4 permanent magnet synchronous machine wind turbine is observed under steady state operation. The voltages and currents at the point of common coupling are as expected. The  $I_d$  and  $I_q$  current values are tracking the reference values closely. In addition the characteristics of a rectifier input and output parameters were explained taking a reference of  $1\phi$  full wave rectifier and mapped to the simulation results of parameters of machine terminals which are connected to a  $3\phi$  diode bridge rectifier.

In the next chapter the fault analysis of the system is done simulating different types of faults, and the simulation results will be analyzed.

## Chapter 5 – Fault Analysis

### 5.1 Introduction

The Type 4 WTG model was developed and tested in simulation as described in the previous chapters. This chapter presents an attempt to analyze the response of the system to faults with the help of simulation results in order to identify reliable fault signatures for protection purposes. Figure 5.1 shows the generic circuit diagram of the test system with a fault at 50% of the length of the transmission line.

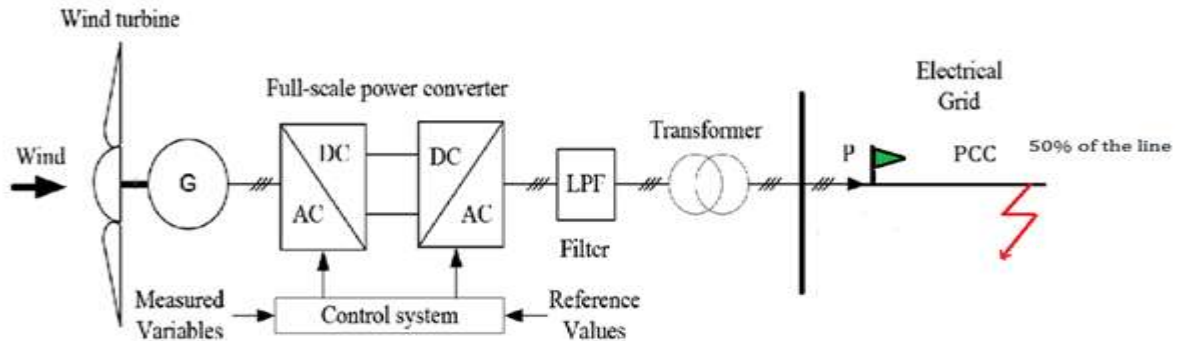


Figure 5.1: Type 4 WTG simulation test system with fault

Two classes of faults will be simulated.

#### Case 1 – Unbalanced faults

- Single Line to Ground Faults (A-G Fault)
- Line to Line Faults (B-C Fault)
- Double Line to Ground Faults (B-C-G Fault)

#### Case 2 – Balanced faults

- 3 Phase Faults (3 $\phi$  Fault)

Before proceeding to the fault simulation, there is one important aspect that needs to be described. When a fault occurs in the transmission line connecting the wind farm with Type 4 turbines to the transmission grid, the voltages and currents at the converter terminals change. But, the magnitude of converter current is limited by the converter controls to stay within the switch current ratings i.e., the maximum amount of current the converter switches can withstand. Sustained over current can destroy the switches. As a result the key measurement feature for developing a new protection scheme is that the magnitude of voltage at the terminals of the converter. The voltage is reduced at the onset of the fault to keep the current constant. Effectively, the exported power is reduced. The power produced by the generator does not change, the difference in power gets stored in the DC link. This action results in a rise in the DC link voltage which might damage the converter switches. There are two ways to overcome this problem to protect the devices. The first is the use of a crowbar circuit which is a set of resistors connected across the DC link through a thyristor switch or an IGBT; dumping the energy to the resistor. Another solution is to add an energy storage scheme to the DC link effectively connecting a set of batteries or larger capacitor banks through a bidirectional dc/dc converters. This dc/dc converter operates when the voltage rises above a threshold, and the energy gets transferred to the energy storage system. The stored energy can be utilized when extra power output is required from the WTG during normal operation. The energy storage could also be used to create synthetic inertia on the power system. In this analysis, a second capacitor bank is connected through back-to-back thyristors and used to model energy storage.

## 5.2 Fault Response Simulation Cases

Faults are simulated at 50% of the length of the transmission line. The measured voltage and current at the point of interconnect are plotted in each of the fault cases.

In each fault case the fault occurs at  $t=0.4\text{s}$  and lasts for a period of 2.5 cycles before the circuit breaker opens. Note that in reality the circuit protection may not respond so quickly. The time window was chosen to challenge the performance of the protection algorithm.

### 5.2a Event 1A: Single Line to Ground Fault (SLG)

Figure 5.2 shows the voltages at the relay location (P) in the Figure 5.1. Figure 5.3 shows the measured current. Note that there is a slight increase in current amplitude, and in ripple, but both are too small to easily distinguish the fault location or fault type. The change voltage due to the fault is more pronounced, and is limited to the faulted phase. There is a slight increase in the voltage amplitude on the unfaulted phases.

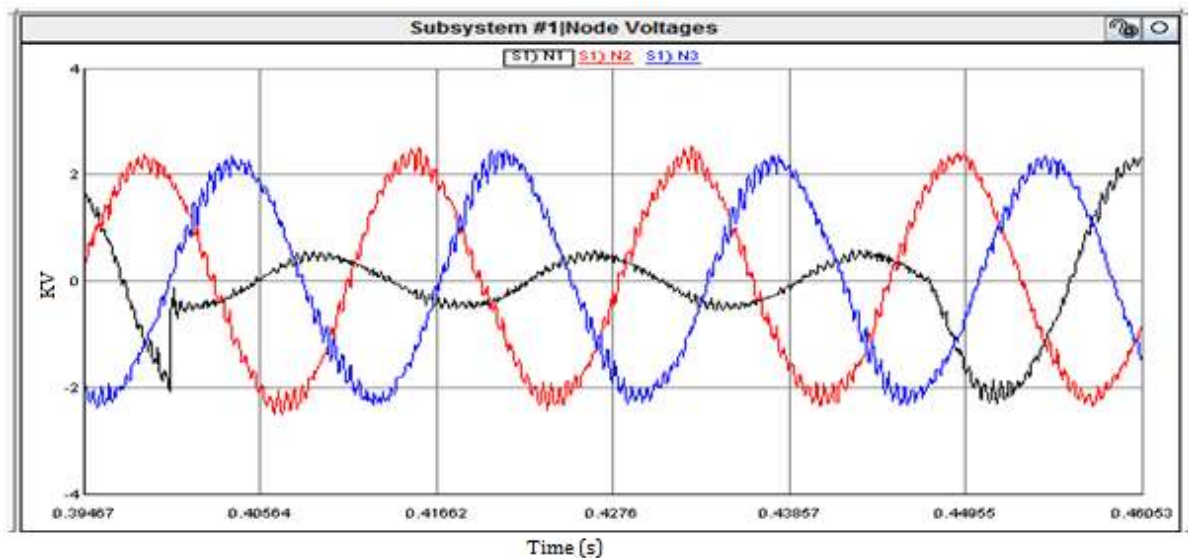


Figure 5.2: Line to ground voltages at relay location - Event 1A

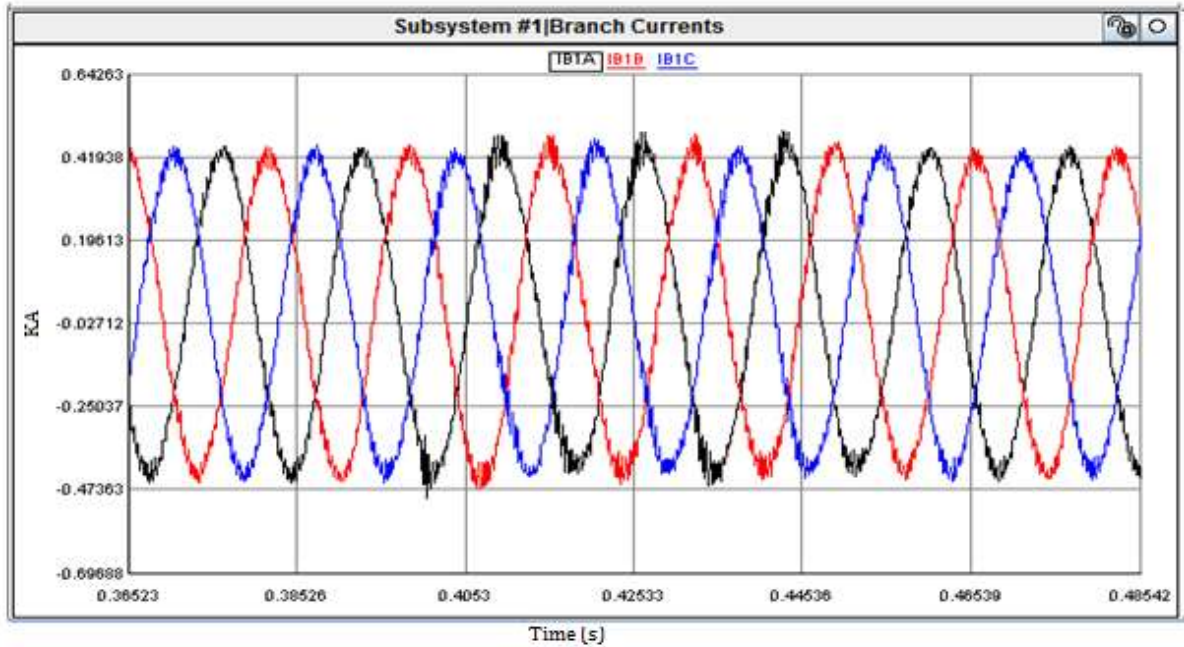


Figure 5.3: Phase currents at relay location – Event 1A

Figure 5.4 shows the fault current. In reality this current cannot be measured in the field. The majority of this current comes from Thevenin equivalent source at the remote end of the transmission line.

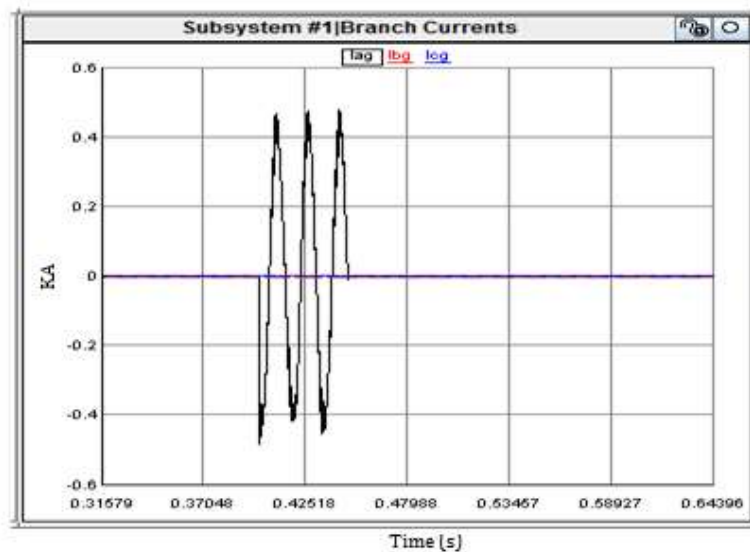


Figure 5.4: Fault current – Event 1A

Figure 5.5 shows the DC link voltage during the fault. Note that there is an increase in the voltage, until crowbar is activated. The crowbar current is shown in Figure 5.6.

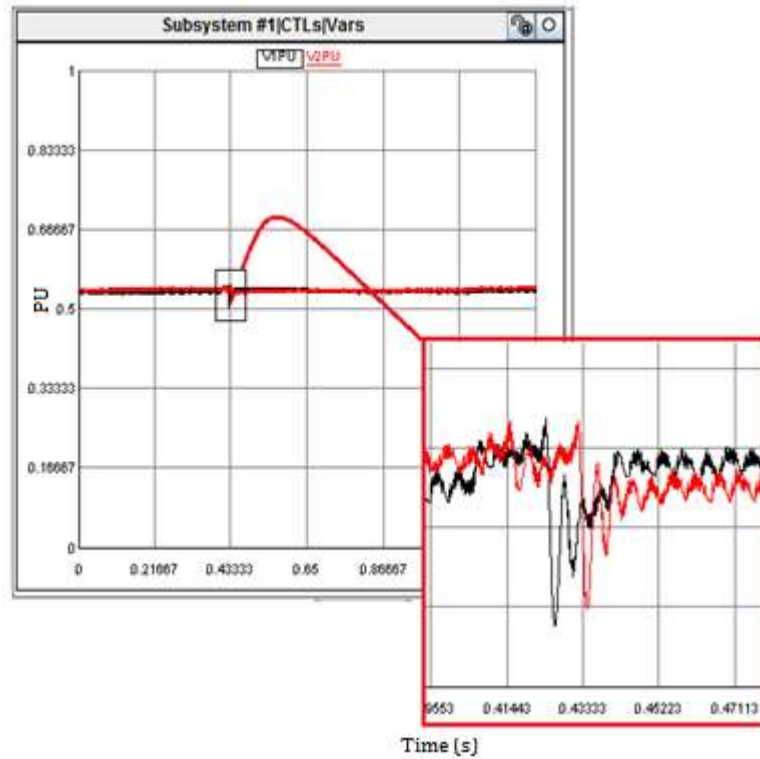


Figure 5.5: DC link voltage – In each capacitor branch (in per unit) – Event 1A

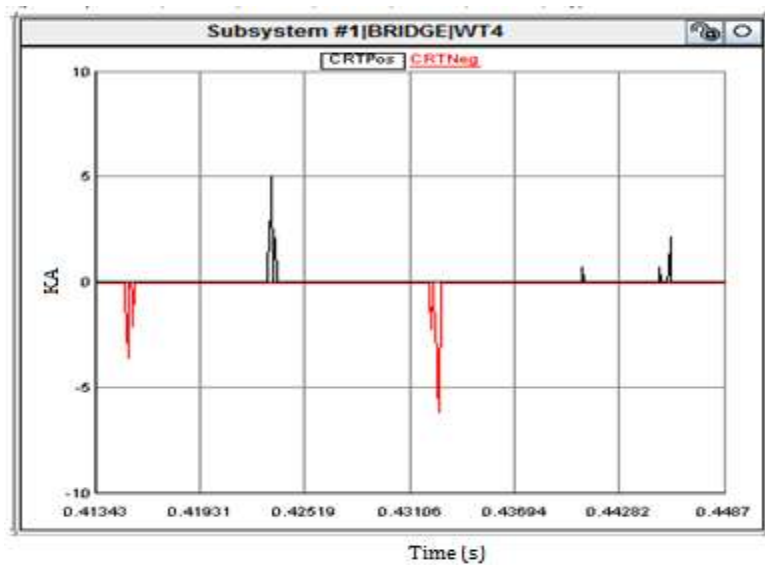


Figure 5.6: Crowbar current for SLG fault

### 5.2b Event 1B: Line to Line Fault (LL)

The second case looks at the response to a LL fault. Figure 5.7 shows the voltages at the relay location (P in Figure 5.1). Figure 5.8 shows the measured current. Note that there is a slight increase in current amplitude, and in ripple, but too small to easily distinguish the fault location or fault type. There is little to visually distinguish Figure 5.8 from the results in Figure 5.3. The change voltage due to the fault is more pronounced, and is limited to the faulted phases.

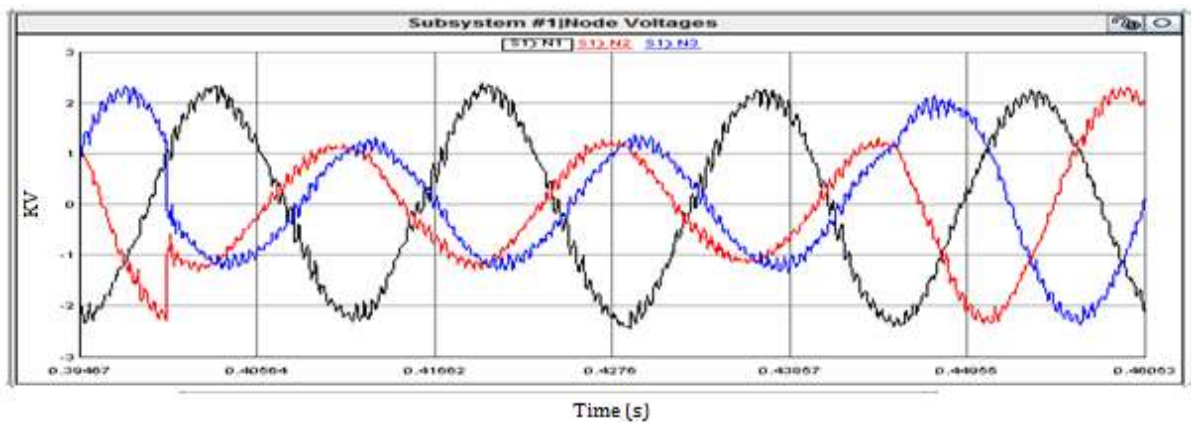


Figure 5.7: Line to ground voltages at relay location– Event 1B

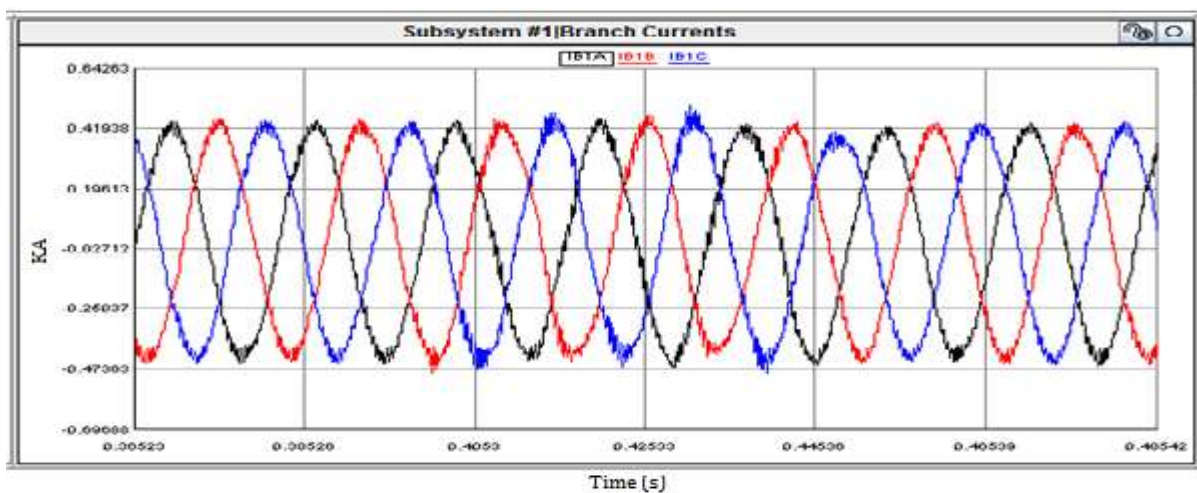


Figure 5.8: Phase currents at relay location – Event 1B

Figure 5.9 shows current flowing through the fault switches. In reality this current cannot be measured in the field. The majority of this current comes from Thevenin equivalent source at the remote end of the transmission line.

DC link voltage and fault current for a LL fault:

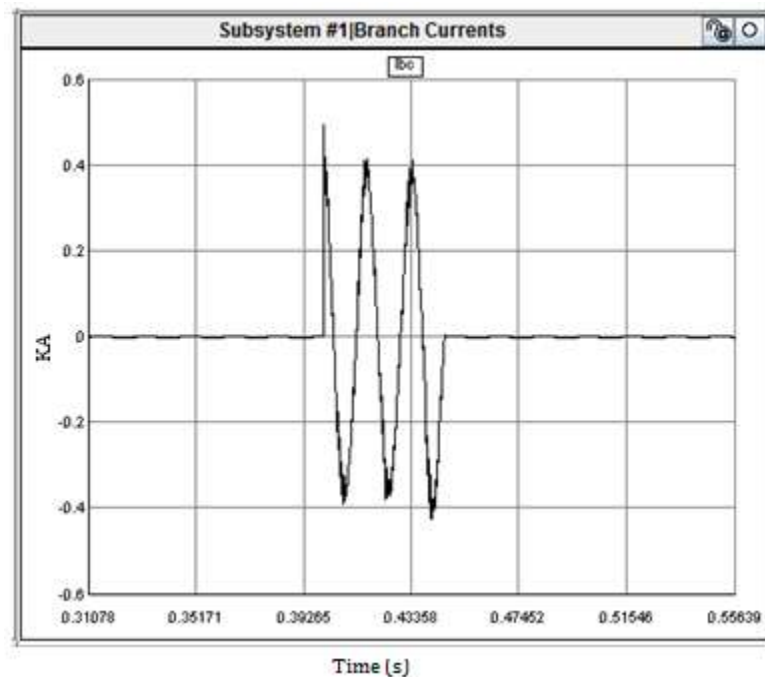


Figure 5.9: Fault current – Event 1B

Figure 5.10 shows the DC link voltage during the fault. Note that there is an increase in the voltage on one capacitor branch and a decrease in the other one, until the crow bar is fired. The crowbar current is shown in Figure 5.11. Again, there is little information to be able to differentiate this response from that shown in Figure 5.5. The most significant change in behavior is shown in the phase to ground voltages.

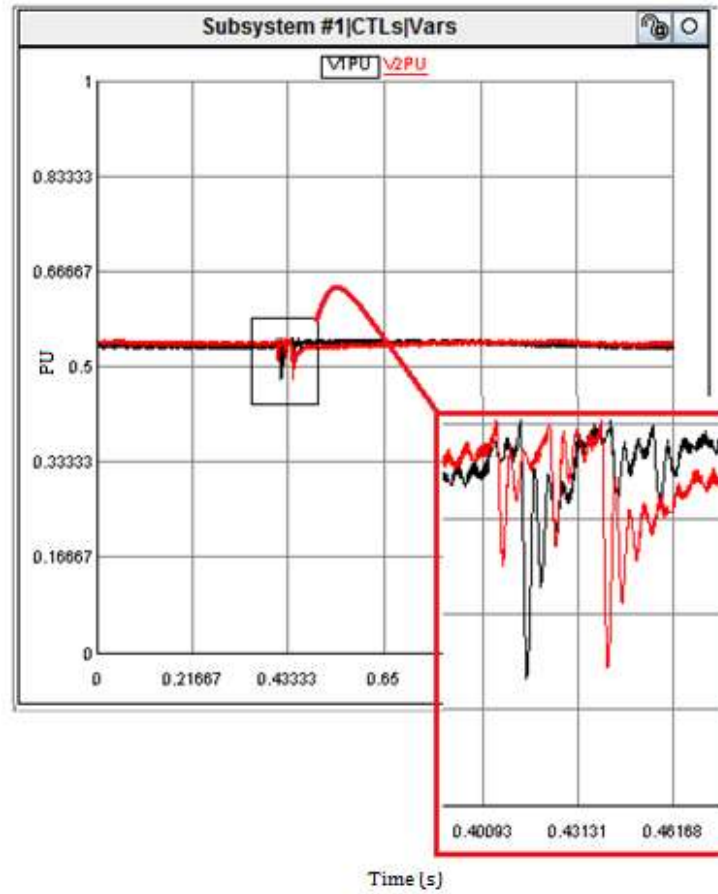


Figure 5.10: DC link voltage – In each capacitor branch (in per unit) – Event 1B

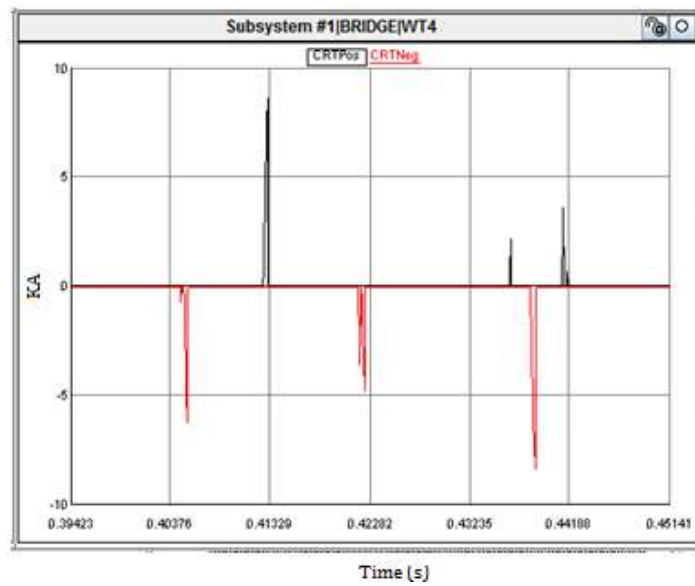


Figure 5.11: Crowbar current – Event 1B

### 5.2c Event 1C: Double Line to Ground fault (DLG)

The third case looks at the response to a DLG fault. Figure 5.12 shows the voltages at the relay location (P in Figure 5.1). Figure 5.13 shows the measured current. Note that there is a slight increase in current amplitude, and in ripple, but too small to easily distinguish the fault location or fault type. There is little to visually distinguish Figure 5.13 from the results in Figure 5.3 or 5.8. Nor would there be much difference if the symmetrical components were calculated and compared. The change the voltages due to the fault are more pronounced, and are again limited to the faulted phases. Note that there is some difference between the DLG and LL fault response.

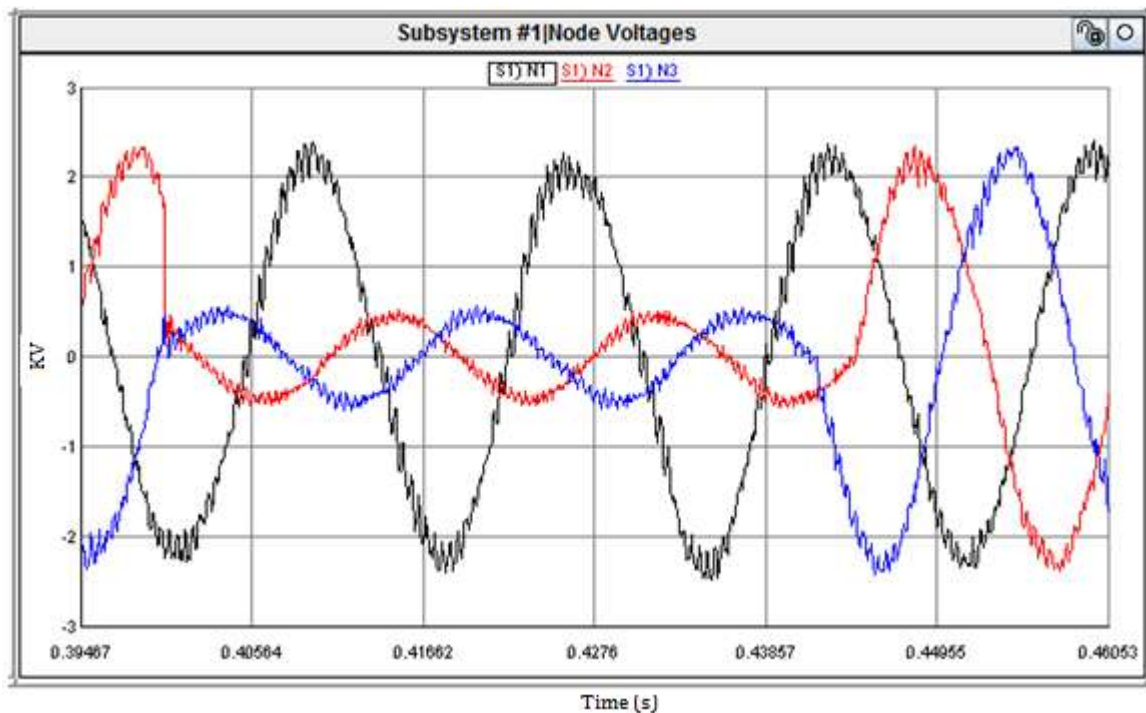


Figure 5.12: Line to ground voltages at relay location – Event 1C

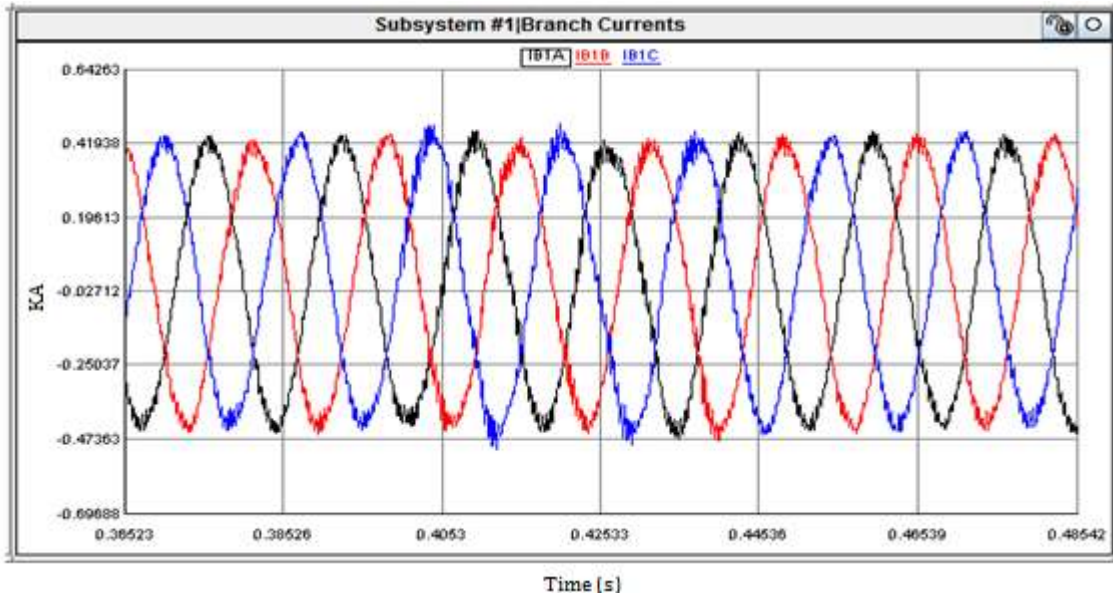


Figure 5.13: Phase currents at relay location – Event 1C

Figure 5.14 shows current flowing through the fault switches. In reality this current cannot be measured in the field. The majority of this current comes from Thevenin equivalent source at the remote end of the transmission line.

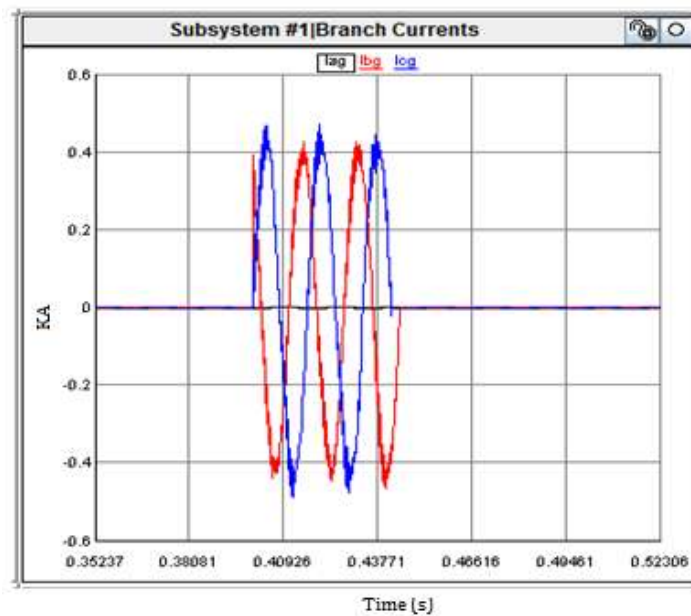


Figure 5.14: Fault current – Event 1C

Figure 5.15 shows the DC link voltage during the fault. Note that there is a transient change in the capacitor branch voltages, until the crow bar is fired. The crowbar current is shown in Figure 5.16. Again, there is little information to be able to differentiate this response from that shown in Figure 5.5 or 5.10. The most significant change in behavior is again shown in the phase to ground voltages.

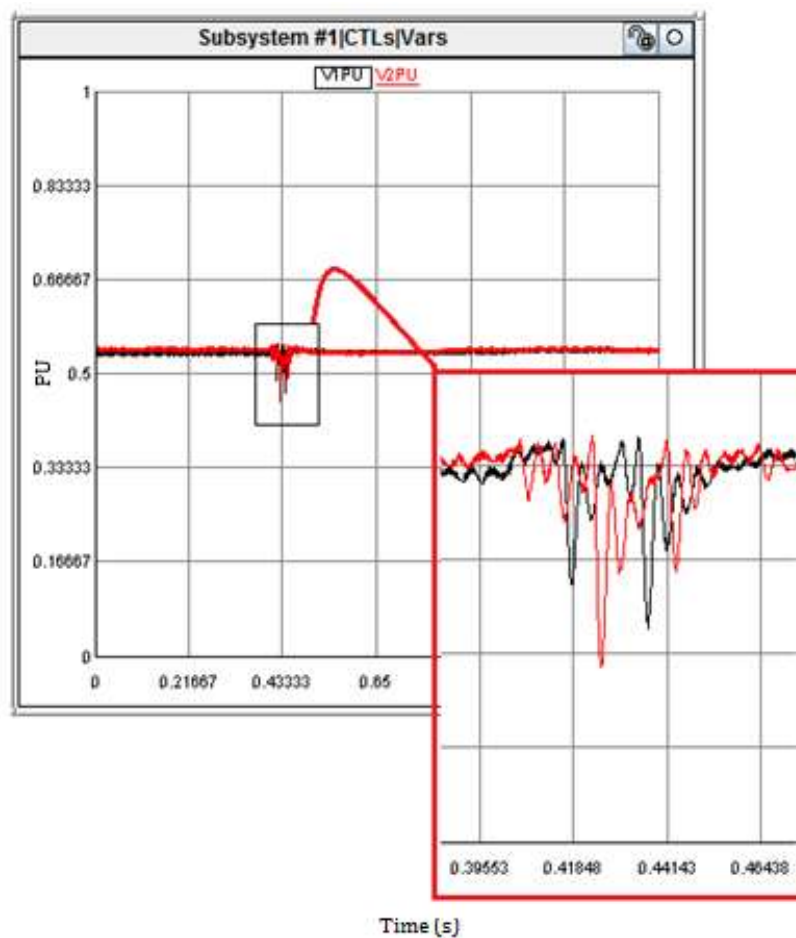


Figure 5.15: DC link voltage – in each capacitor branch (in per unit) – Event 1C

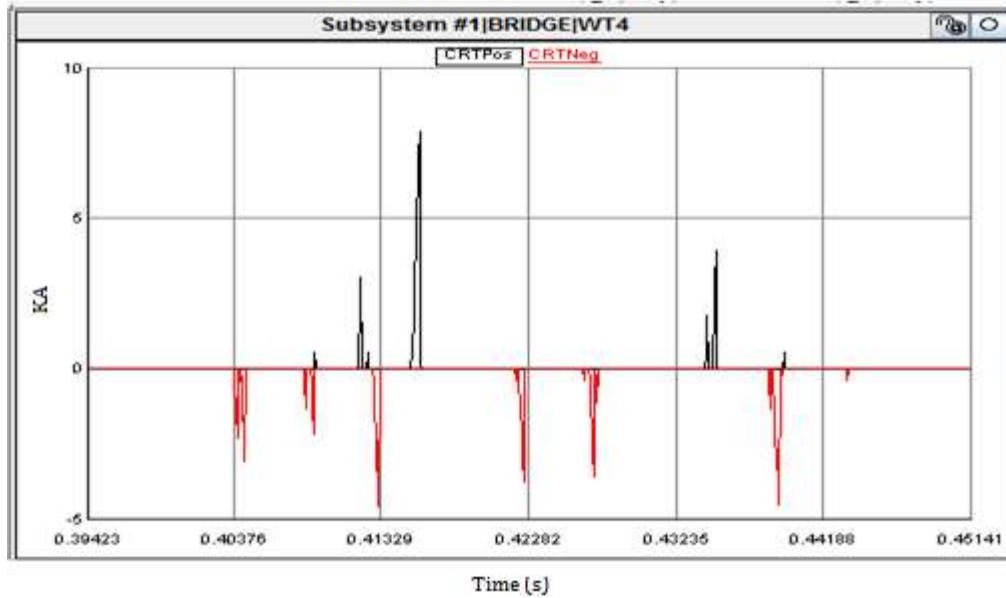


Figure 5.16: Crowbar current – Event 1C

#### 5.2d Event 2: Three phase fault at 50% of the line

The fourth case looks at the response to a three phase fault. Figure 5.17 shows the voltages at the relay location (P in Figure 5.1). Figure 5.18 shows the measured current. Note that there is a slight increase in current amplitude, and in ripple, but too small to easily distinguish the fault location or fault type. There is little to visually distinguish Figure 5.15 from the results in unbalanced fault cases. The change the voltages due to the fault are more pronounced, and are again limited to the faulted phases.

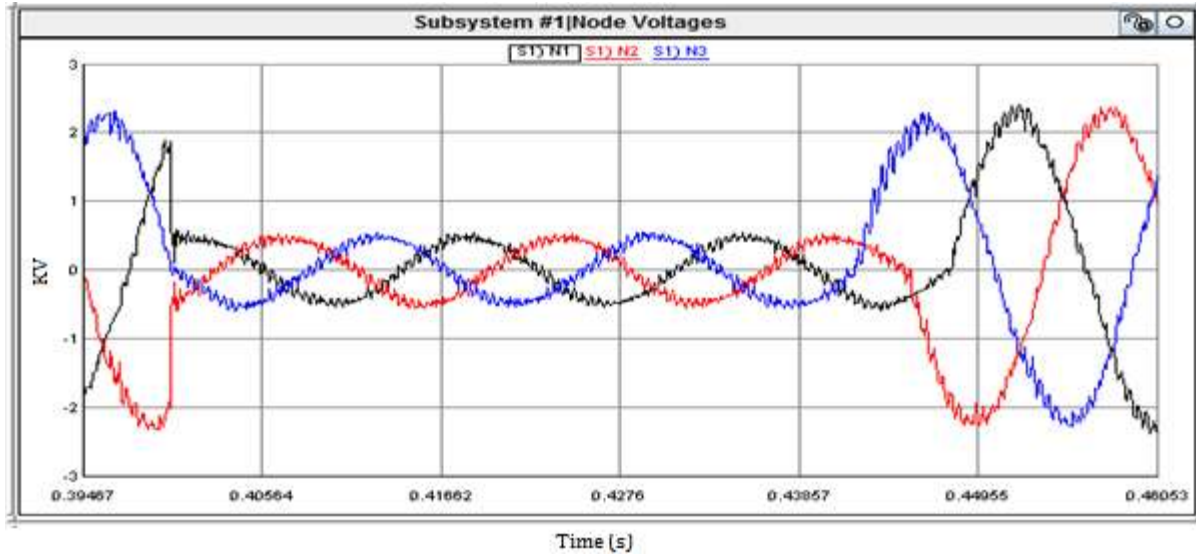


Figure 5.17: Line to ground voltages at relay location – Event 2

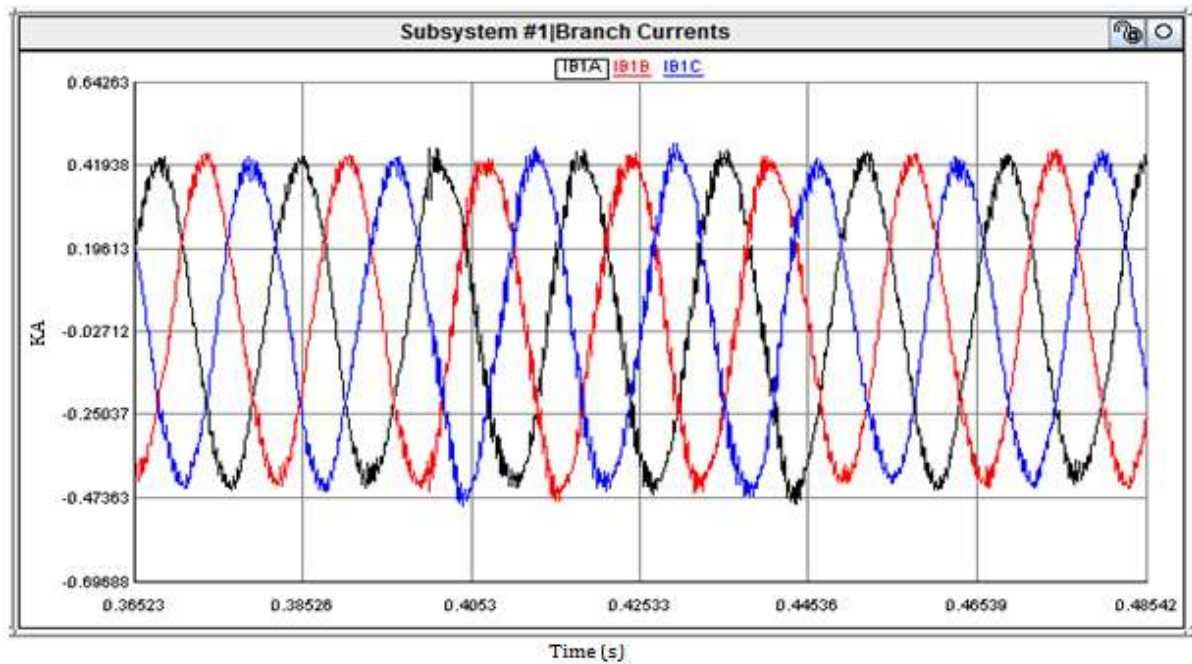


Figure 5.18: Phase currents at relay location – Event 2

Figure 5.19 shows current flowing through the fault switches. In reality this current cannot be measured in the field. The majority of this current comes from Thevenin equivalent source at the remote end of the transmission line.

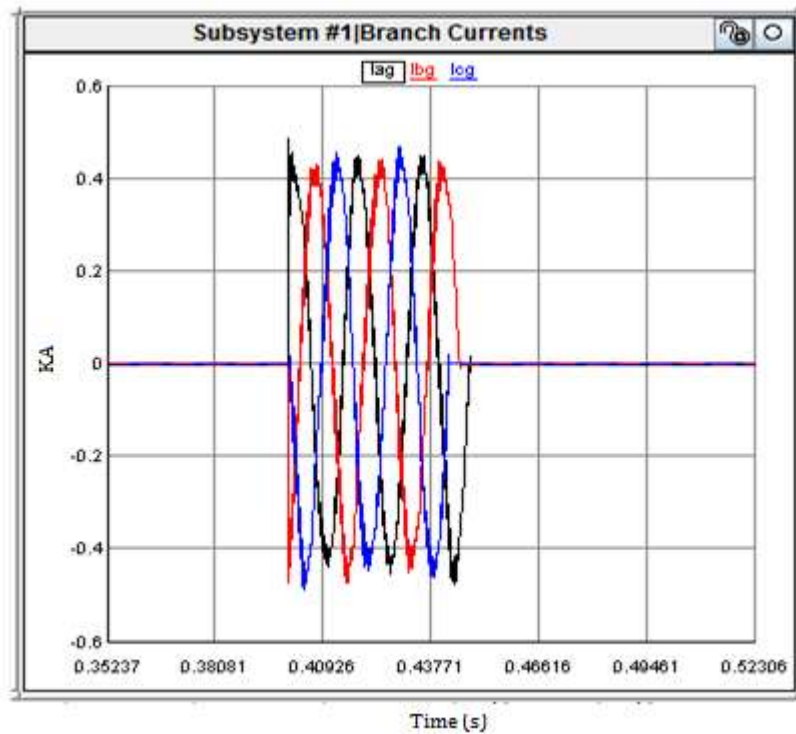


Figure 5.19: Fault currents – Event 2

Figure 5.20 shows the DC link voltage during the fault. Note that there is an increase in the voltage on one capacitor branch and a decrease in the other one, until the crow bar is fired. The crowbar current is shown in Figure 5.21. Again, there is little information to be able to differentiate this response from that shown in the earlier cases. The most significant change in behavior is shown in the phase to ground voltages.

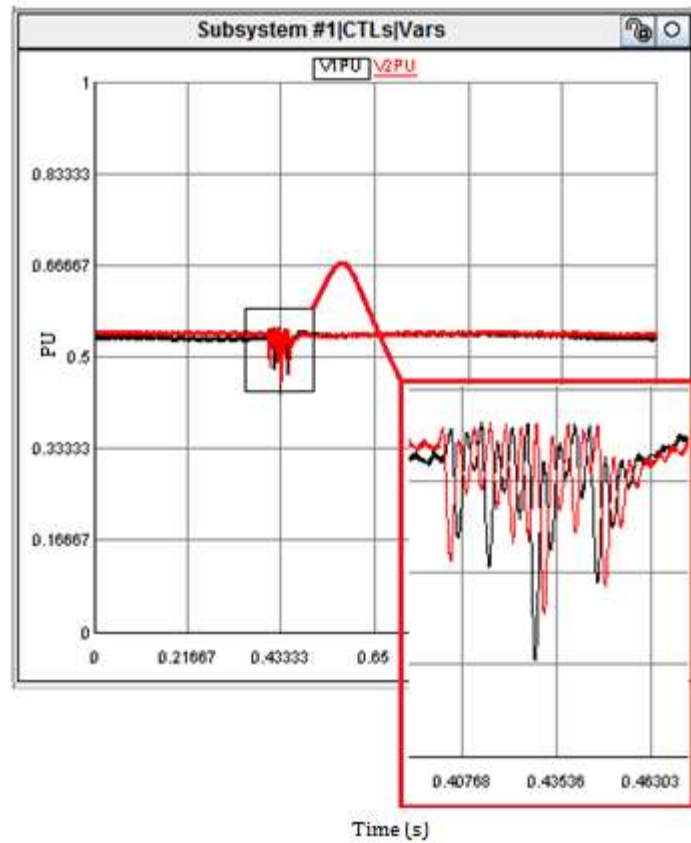


Figure 5.20: DC link voltage – in each capacitor branch (in per unit) – Event 2

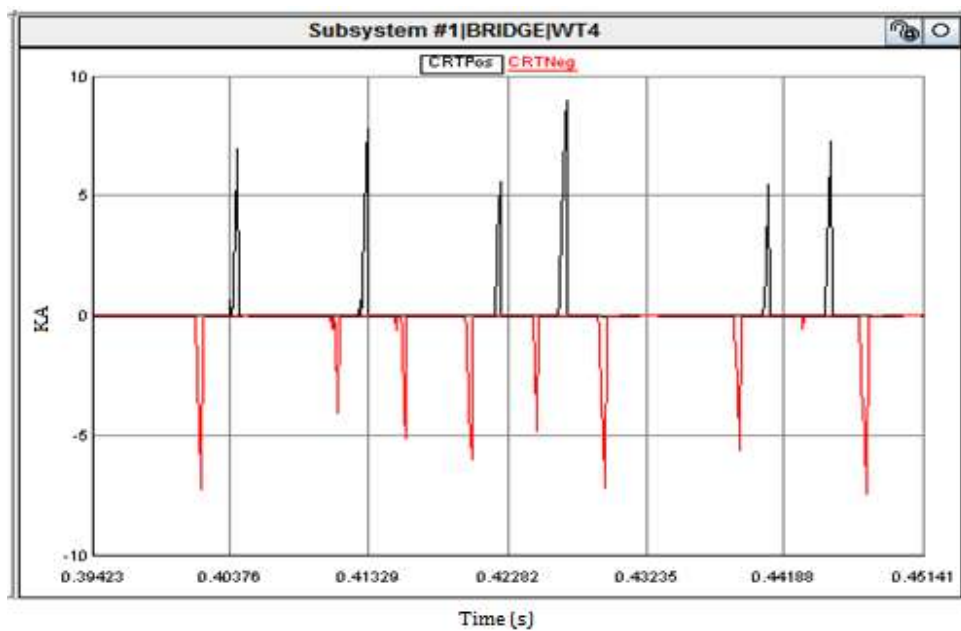


Figure 5.21: Crowbar current – Event 2

### **5.3 Conclusions Drawn**

The voltage waveforms demonstrate the indirect impact of the controller reacting to the fault by varying the magnitude of converter terminal voltages to keep the current within limits when there is a fault in the system. The current supplied by the wind turbine is almost constant, there is a only slight change in the current in response to the fault since the controller is reacting fast to bring the current within the set limits. The reaction time of the controller is measured in switching periods. The disturbance can also be sensed through the DC link voltage, although that is not readily available to the transmission relay. Note that there is a change in DC link voltage for any kind of disturbance, but there isn't a clear signature differentiating different fault types.

### **5.4 Summary**

This chapter showed the responses for various types of faults. The variation of ac voltages and currents, DC link voltage and fault currents for both balanced and unbalanced faults were shown.

In the next chapter the limitations of conventional protection schemes for use with Type 4 WTG systems are discussed.

## Chapter 6 – Response of Existing Protection Schemes and Protection Limitations

### 6.1 Introduction

In the case of a wind farm covering a region with multiple wind turbines spread over a large area, all the turbines in the farm might not operate at the same operating conditions. Some of the turbines might be off line due to low load wind speed. The line protection scheme applied must react correctly when transmission faults occur under all types of wind variations and operating conditions.

The basic role of protection schemes/relays is to sense an abnormality in the part of the system they are protecting, identify whether the abnormality is due to a fault in its protective zone, and assert if the results are positive. There are various types of relays that are employed for providing protection to lines connected to wind farms. The authors of [21] describe basic protection schemes and their underlying principles of operation.

### 6.2 Overcurrent relay

An overcurrent relay is a level comparison type of protective relay, which operates when the current exceeds a preset pick up value. The ANSI notation for this element is 50/51 for an Instantaneous Overcurrent (IOC)/Definite Time Overcurrent (DTOC) relay. They are connected to the secondary of current transformers and are calibrated to operate at or above a specific set reference value called a pick up setting. When a situation arises where the current exceeds the trip threshold, the element generates a trip command that is sent to the breaker trip coil. Let  $I_{op}$  be the measured value and  $I_{rtpu}$  be the restraint value, or pick up value.

$$\text{If } I_{op} > I_{rtpu} \text{ -----} \rightarrow \text{Trip} \quad (6.1)$$

In case of fault supplied by a Type 4 WTG converter, the converter is designed such that the current output doesn't exceed 1.1 pu due to the current rating of the switches, as discussed in Chapter 5. When a fault occurs beyond the PCC, the controller adjusts amplitude and phase of the converter modulating wave reducing the voltage at the converter terminal in order to keep the current magnitude within the limit and maintain power factor. As a result, an overcurrent element cannot be applied to provide reliable protection for a wind farm with Type 4 WTGs. If it is employed, such elements are unlikely to generate a trip command and the relay misoperates.

### 6.3 Under Voltage Relay

An under voltage relay is also a level comparison type protective relay which operates when the voltage falls below a preset pick up value. The ANSI notation for this relay element is 27. The voltage measurements come from a potential transformer. The element is calibrated to generate a trip command to the breaker when the voltage falls below a certain level. Let  $V_{op}$  be the value of measured voltage and  $V_{pu}$  be the pickup value.

$$\text{If } V_{op} < V_{pu} \text{ -----} \rightarrow \text{Trip} \quad (6.2)$$

In the case Type 4 WTG connected to a system with a weak source at the other end of the transmission line, there is potential for significant voltage variations with wind speed. In such cases, alternative reactive power sources are operated or load shedding is done which requires a certain time interval for operation. So if this relay is used for

protection at the Point of Interconnect, it might misoperates, disconnecting the source from the system.

#### **6.4 Differential Relay**

A differential relay is one that operates when there is a difference between two or more similar quantities that exceeds a predetermined value. In a current differential scheme the two currents measured on both sides of the protected apparatus are connected using wires or a communication circuit. According to Kirchhoff's current law the resultant current has to be close to zero under normal load currents or external faults. In effect the current input to the device has to be equal to current going out of the device, with no other connections that aren't monitored. If a fault occurs in the protected zone, the differential current becomes non-zero. The main logic behind the differential scheme is that it senses the faults by monitoring the differential current. In microprocessor relays this is implemented by comparing the phasor values. "The differential protection is 100% selective and therefore only responds to faults within its protected zone. The boundary of the protected zone is uniquely defined by current transformers. Time grading with other protection systems is therefore not required, allowing for tripping without additional delay. Differential protection is suited as fast main protection for all important plant items." [21].

A differential scheme is a good option for protecting lines connected to wind farms with 4 WTG systems. But as previously stated, the system up to the Point of Interconnect is owned by the wind farm owner and from that point onwards, it may be in the hands of utilities. Hence to get the values from other end of the line, a dedicated

communication line is needed, which is sometimes not possible. This protection scheme cannot be applied in situations where communication is not available. In addition, the fault current at the wind farm end of the line may fall below the minimum pick up level for the differential element in cases where a small number of WTGs in a large farm are operating [22].

### 6.5 Distance Relay

A distance relay operates based on the effective impedance between the fault point and the relay location, calculated from the values of voltages and currents. These relays are also known as impedance relays. The ratio of voltage from potential transformer to current from the current transformer is compared to a predetermined set value. If the effective value falls below the restraint value, a trip command is issued for the breaker. Let  $V_{oper}$  and  $I_{oper}$  be the measured operating voltages and currents respectively. The calculated impedance  $Z_{calc}$  is as shown in (6.3).  $Z_{ref}$  is the value of  $Z_{calc}$  under normal operating conditions.

$$Z_{calc} = \frac{V_{oper}}{I_{oper}} \quad (6.3)$$

$$\text{If } |Z_{calc}| < |Z_{ref}| \text{ ---} \rightarrow \text{Trip} \quad (6.4)$$

An impedance type relay operates for the faults in reverse direction also. To overcome this, a modified impedance relay was developed by offsetting the setting threshold to give the element a directional bias. This relay compares the operating quantity with the polarizing quantity and determines the direction of the fault. It can be represented in a graphical form as shown in Figure 6.1.

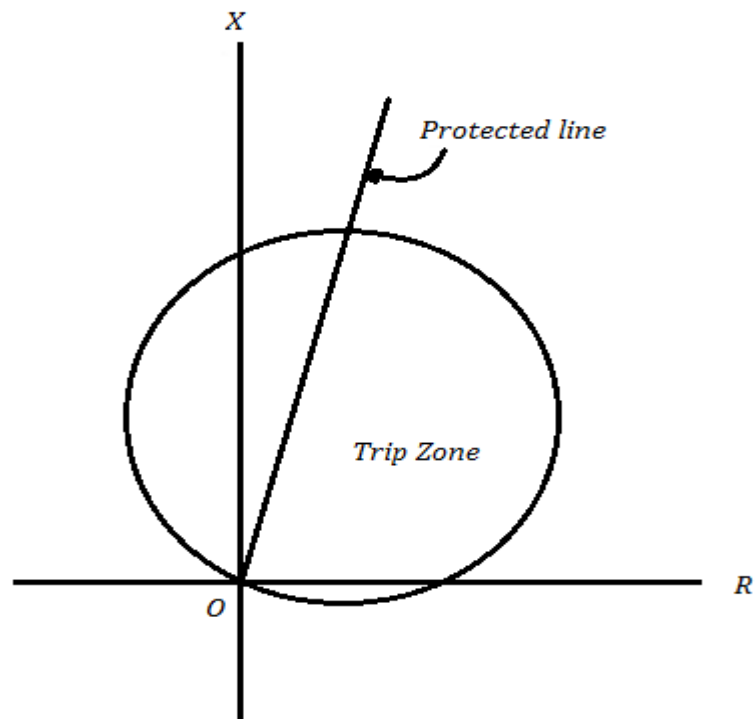


Figure 6.1: Impedance Relay Characteristic

The trip command is issued only if the fault is inside protection zone. A polarizing quantity is a value that remain unchanged for different faults. This polarizing quantity may be a voltage, voltages from other phases, or the output from a memory filter. To improve the security of the distance element, the trip command is supervised with a directional element. For unbalanced faults this supervision is done using a negative sequence or a zero sequence directional element.

In the case of a wind farm with Type 4 WTGs, the currents are limited and are balanced even for unbalanced faulted conditions. Negligible negative sequence or zero sequence current flows from the converter. The WTG cannot be modeled as a source behind impedance in the positive sequence. It can be considered as a variable source keeping the current constant maintaining a constant power factor. For such a situation

the directional supervising element fails to qualify the fault as forward and the relay will misoperate.

## **6.6 Summary**

In this chapter, various protection relay schemes and their operating principles were explained, along with reasons that could cause the relay to misoperate if used for providing protection for lines connected to Type 4 wind farms.

A new scheme that can be used for protection in such cases is derived and explained in the next chapter.

## **Chapter 7 – Proposed Protection Scheme**

### **7.1 Introduction**

In the previous chapter, it was concluded that certain conventional protection schemes are not reliable in providing protection to transmission lines connected to Type 4 WTG systems. Based on the fault response of the system, the following schemes could be considered to provide protection, but they are not adequate.

- DC link voltage: It is clearly observed that the DC link voltage varies for different types of faults. This response can be used for fault detection, but the type of fault, distance to fault or the faulted phases cannot be determined using the change in DC link voltage.
- Transients induced by the fault: There are transients induced in the transmission line due to the sudden change in the voltage based on the characteristics of the transmission line. Transients can be detected when the fault occurs at a nonzero voltage. It will be difficult to sense transients if the fault occurs at a point on the voltage waveform near a voltage zero.

Therefore, an additional scheme that works under all conditions is needed.

### **7.2 New Protection Scheme**

As discussed in Chapter 5, the voltage at the PCC varies as the converter controller varies the converter output voltage to keep the current constant at the point of interconnect. Before the fault, the effective impedance looking into the system is high and the current supplied is at unity power factor. If a fault occurs in the system, the magnitude and phase of the modulating wave changes to keep the current less than

current threshold, which is typically around 1.1 pu. Since the fundamental component of the terminal voltage is a scaled version of the modulating wave, the change is seen in the terminal voltage. In addition, a change in the voltage at the PCC will also be seen, although less clearly. This change in voltage can be used to identify the fault and protective measures can be taken (issuing the trip signal to the breaker).

The variation of voltage magnitude at the PCC for various faults discussed above will be observed in the simulation studies in Section 7.3. Generally in case of a microprocessor relay, the output from the potential transformer is fed to a loop with an anti-aliasing filter, an A/D converter, and a Fourier filter. The gain of a Fourier filter or a cosine filter is unity at fundamental frequency, and is zero for all the integer harmonics of the fundamental quantity (provided it is a one cycle cosine filter). The anti-aliasing filter attenuates the higher frequency components. The final output values of the filter will then be used for processing. The simulation responses for this thesis are dealt with a similar fashion. The simulated ac voltages are processed through a down sampler with linear interpolation then fed to a band pass filter of range 59 – 61 Hz. Then the RMS values of the output waveforms are calculated and scaled to per unit. The final output waveforms are studied in Section 7.3. Relay is located at P shown in Figure 7.1.

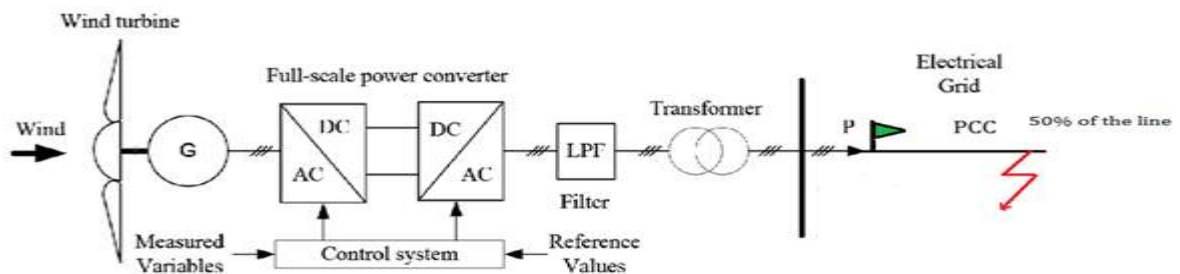


Figure 7.1: Type 4 WTG simulation test system with fault

### 7.3 Simulation Results

#### Event 1A: SLG fault at 50% of the line

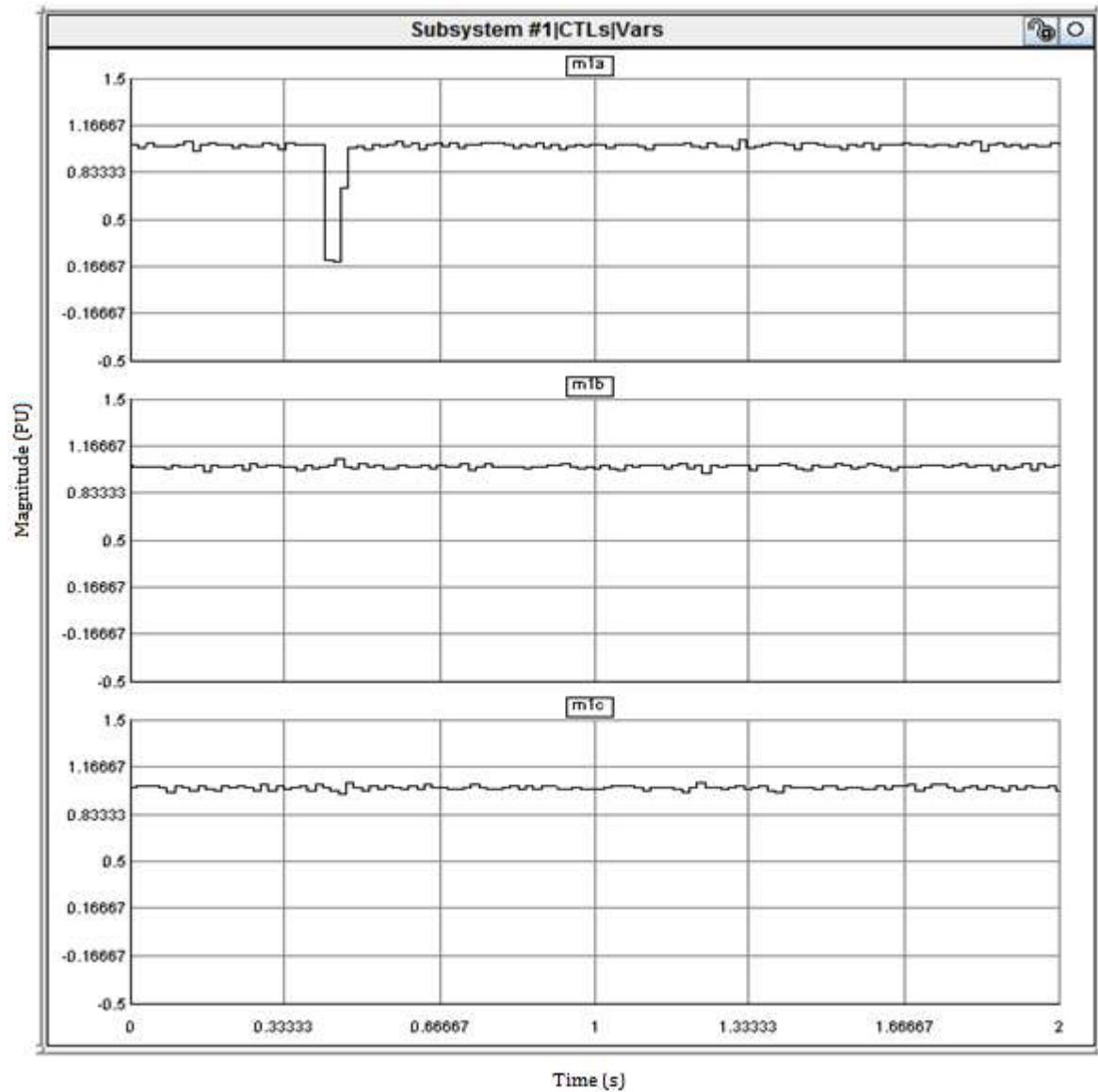


Figure 7.2: Calculated RMS voltage magnitude at the relay location – Event 1A

When the fault occurs in phase A, the effective impedance of the faulted phase seen by the relay will be the impedance of the transmission line up to the fault point. The converter controller varies effective line to ground voltage of the faulted phase in such a

way that the fault current is kept down to 1.1 pu, nearly equal to the other phases. As shown in Figure 7.2, only the faulted phase sees a change in voltage.

Event 1B: LL fault at 50% of the line

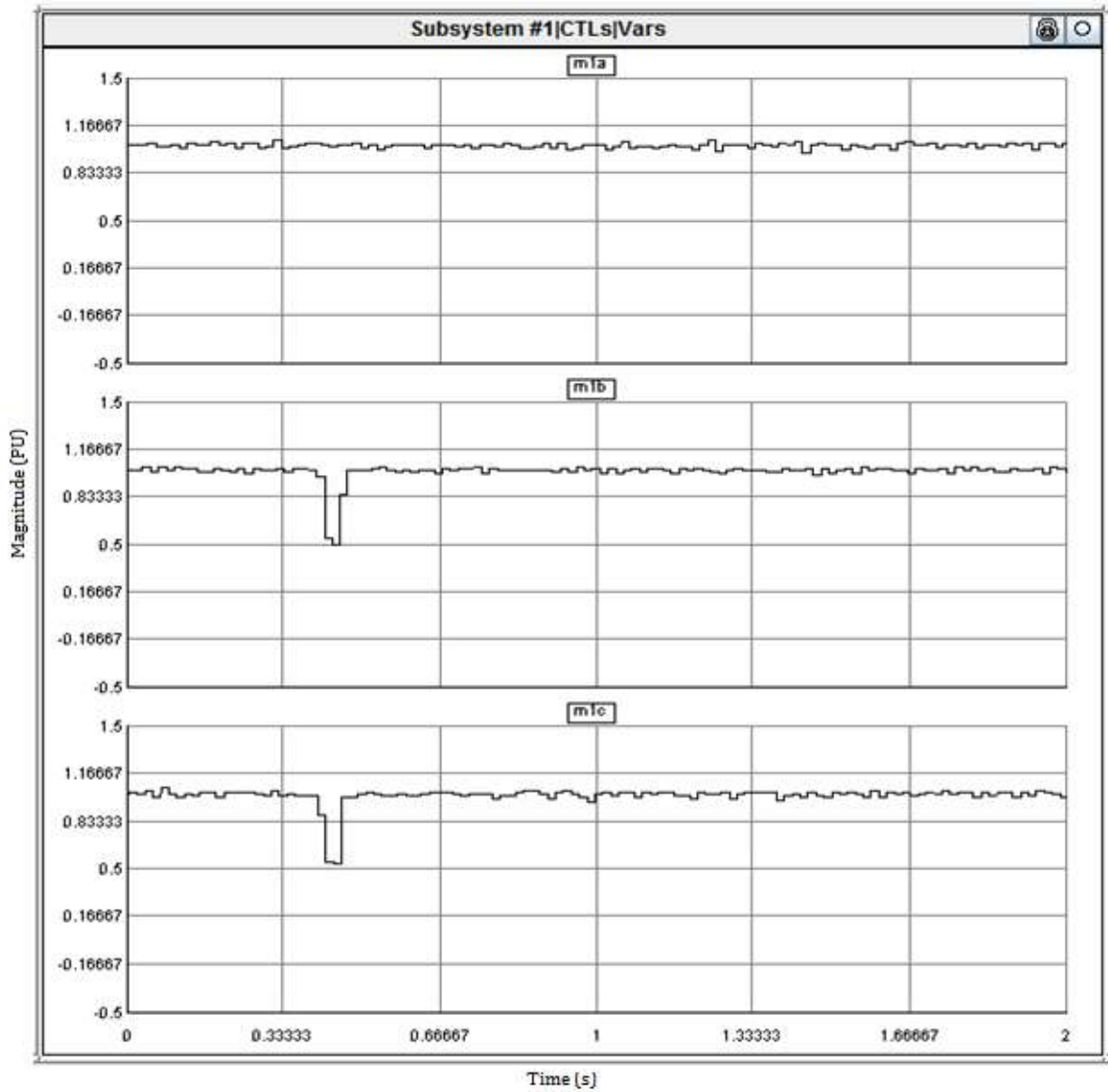


Figure 7.3: Calculated RMS voltage magnitude at the relay location – Event 1B

In the case of the LL fault in Figure 7.3, the instantaneous magnitude of the line to ground voltages on phases are reduced for a BC line to line fault. The phase A voltage is almost unaffected.

Event 1C: DLG fault at 50% of the line

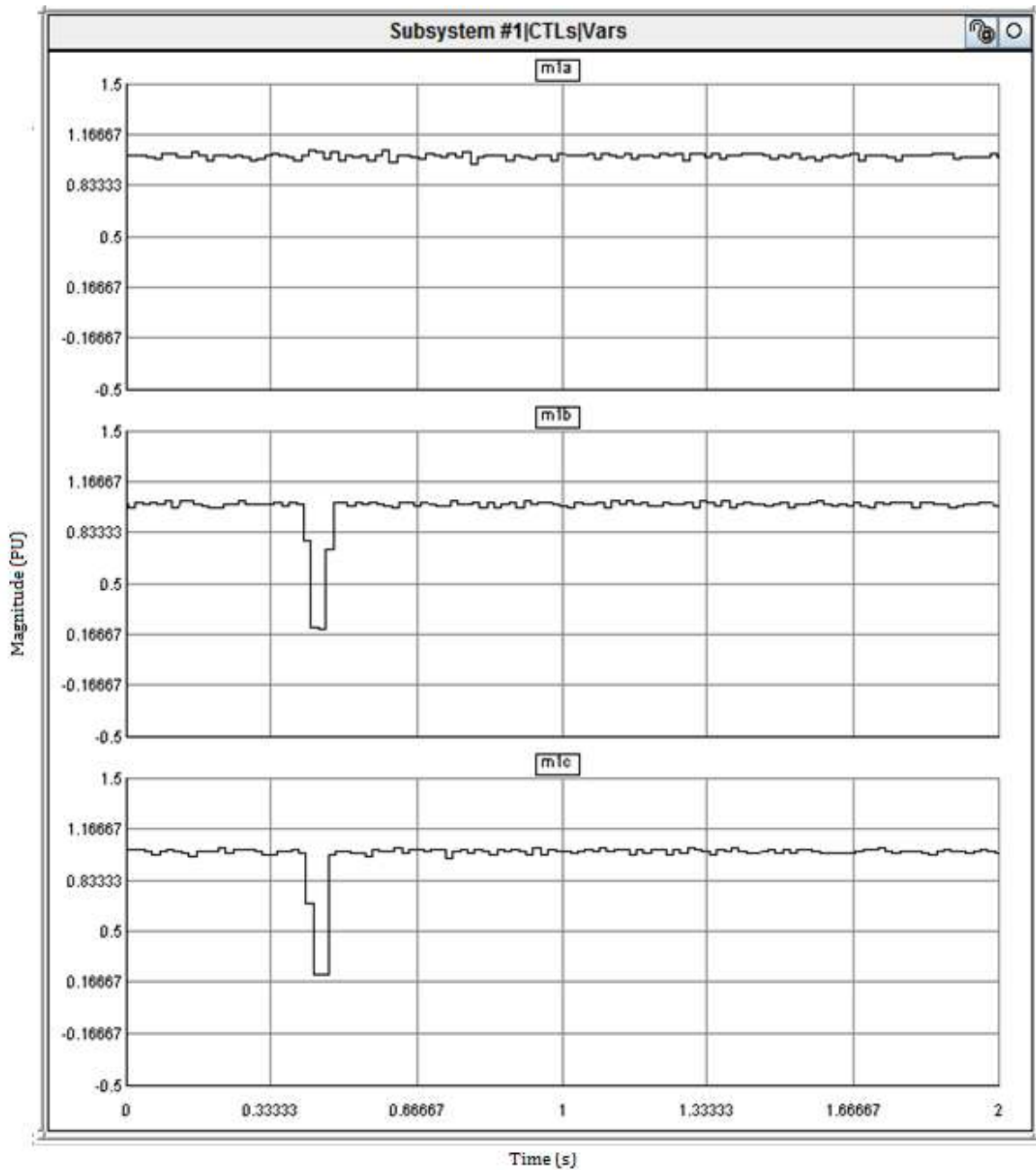


Figure 7.4: Calculated voltage magnitude at the relay location – Event 1C

Figure 7.4 shows that the magnitudes of the line to ground voltages on the faulted phases are again reduced for DLG fault and look similar to the LL fault case, but there is a larger change in magnitude. This voltage dip is same as the SLG fault in each phase when there is no fault resistance.

### Event 2: Three phase fault

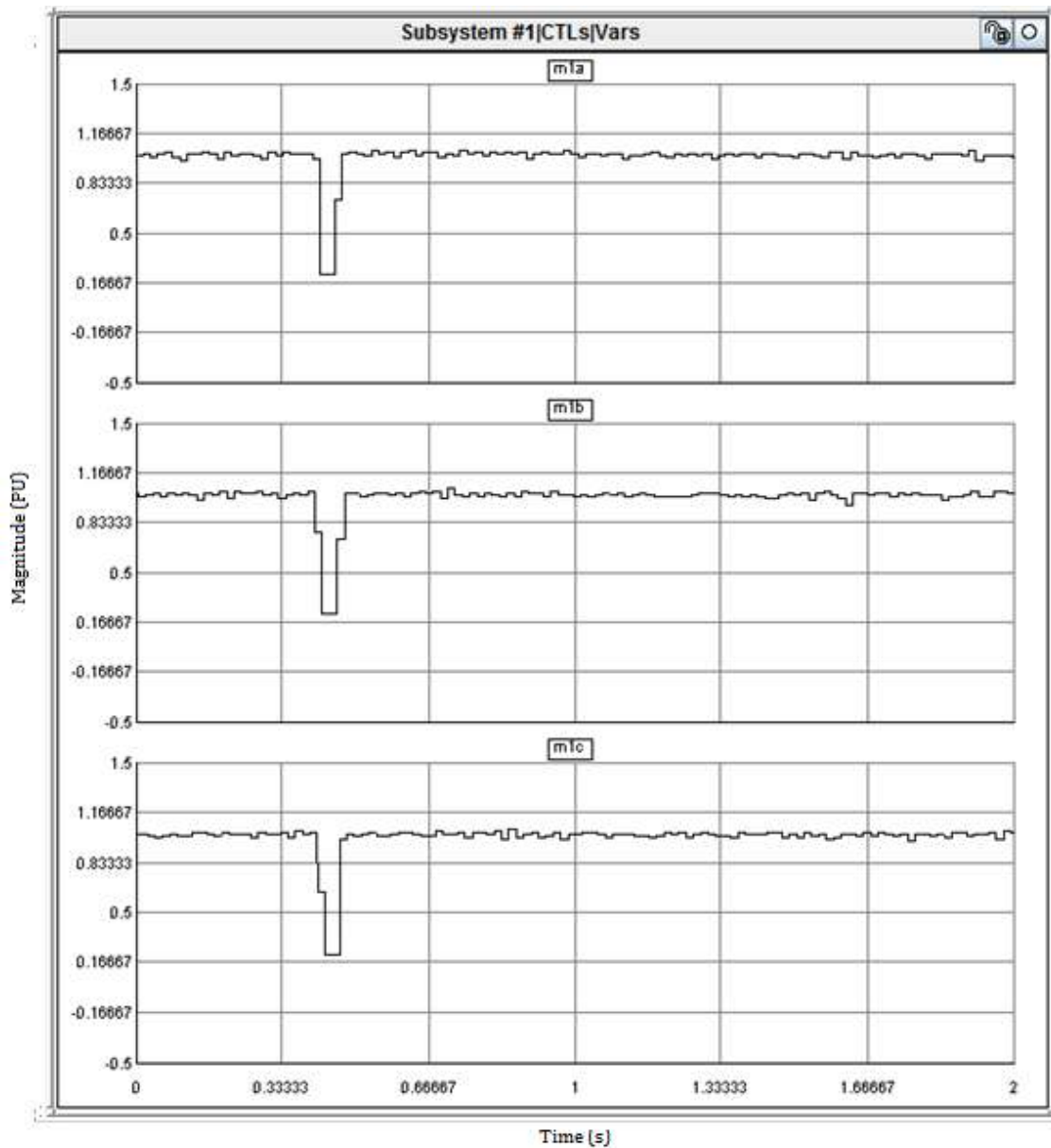


Figure 7.5: Calculated voltage magnitude at the relay location – Event 2

For a 3 phase fault, all the three phases experienced the dip in the magnitude. This dip is same amplitude as the previous ground faults at the same fault location but in all three phases.

#### 7.4 Impact of Fault Location and Fault Resistance

Many additional cases were also simulated, including faults at different locations on the transmission line and faults with varying fault resistance.

It is observed that the dip in voltage magnitude is proportional to the percent length of the line to the fault point. Figure 7.6 shows effective voltage magnitude the plotted for different fault locations.

Table 7.1: Modulating wave magnitude for different fault length,  $R_f=0$

Fault at % distance	Magnitude
1	0.025
25	0.125
50	0.2146
75	0.2925
100	0.3935

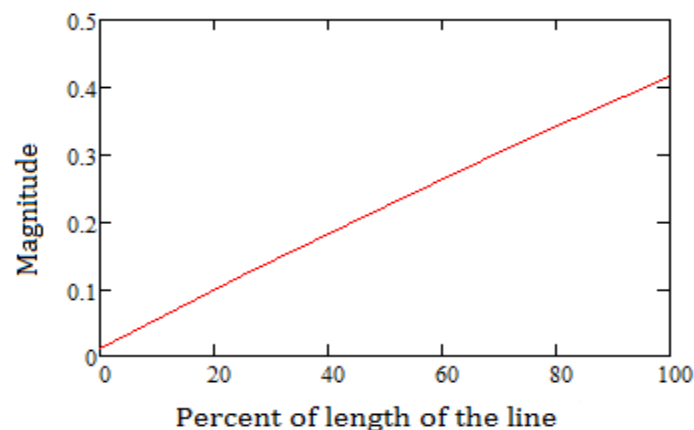


Figure 7.6: Length of line to the fault point versus Modulating wave magnitude

The results of Figure 7.6 show that for solid faults with no fault resistance, the dip in voltage magnitude is nearly proportional to the distance to the fault point. The slight magnitude at 0% of the transmission line is the on state voltage drop across the circuit breaker. So, an additional advantage of this approach is that the approximate fault location can be determined using the dip in magnitude.

Fault location calculation might not give accurate fault location if there is a fault resistance involved; the dip in voltage gets reduced due to the potential at the fault point on the transmission line. If the fault resistance is high the change in voltage magnitude is small, especially if the remote source is stiff. For the study system used in this work the total positive sequence impedance of the line was  $2 + j0.075$  ohms and the fault resistance of 24 ohms, resulted in a change in voltage magnitude of less than 5%.

## **7.5 Summary**

In this chapter, the basic performance of a new protection scheme for lines fed by Type 4 WTGs was proposed and tested using transient time domain fault simulations. This scheme works for all types of systems and conditions including a wide range of operating conditions.

In radial system the voltage might drop if the loading on the wind farm increases where the only source of power to the loads at the other end of line is the WTGs. This may cause a relay misoperation. This problem can be rectified by taking the current values.

The limiting factor for the scheme is the sensitivity with fault resistance and remote infeed. It is possible to overcome this problem to an extent, if the relay signals remain within its sensitivity limit.

## **Chapter 8 – Summary, Conclusions and Future Work**

### **8.1 Summary**

With the rise in demand for clean energy sources, installation of wind energy systems is increasing rapidly. The behavior of wind turbines under fault conditions is important for designing protection schemes. Detailed information about the control behavior will not be provided by the manufacturers. An attempt to clearly visualize the controls is made in this research. The results show that with the variation in operation of a Type 4 WTG at varying wind speeds and different fault conditions, the response of the turbines cannot be considered equivalent to that of conventional energy sources, confirming results in the literature. Type 4 wind turbine systems can be treated as controlled current sources that change their voltage characteristics to operate the system within the rated conditions to protect the power electronic devices.

### **8.2 Conclusions**

The fault current contribution changes little for different wind speeds but in almost all cases the fault current will be almost equal to the pre-fault current. The faults simulated at different points of the transmission line gave a good insight into the effects on WTG response. A few operational and sensitivity challenges of the protection schemes were discussed. The conclusions that can be drawn from the simulation results are:

1. The Type 4 WTG system cannot be modeled as a voltage source behind a reactance. The source voltage magnitude and angle changes according to the conditions to limit the current, unlike the case with synchronous generators.

2. The source voltage varies in such a way to keep the current within 110% of rated load current.
3. The balanced current implies that there is negligible negative sequence or zero sequence currents provided by the WTG system during the fault.
4. Overcurrent protection cannot be applied since the current in the system is kept nearly constant in pre-fault and post fault conditions.
5. An under voltage relay misoperates if the system is radial or when the grid side source is a weak source.
6. A differential relay can be used for the operation but needs a dedicated communication line plus a backup communication line. Line current differential protection also fails to operate when there is loss of communication.
7. The fault current contribution from a large wind farm may not be sufficient to meet minimum operation for a line current differential relay if a small number of wind turbines are operating.
8. The operation of the differential relay will be different if the source on the grid side is a weak source.
9. A distance element could misoperate because directional supervision elements may block a trip command.
10. The DC link voltage can be used to identify that a fault has occurred, but cannot be used to find the faulted phase or phases.
11. The transients in the line with the change in voltage due to the faults can be used to determine the faults, but there will be no transients if the fault occurs near a voltage zero.

In response to these limitations, the proposed scheme based on the reduction in magnitude of the point of interconnect voltage works for all wind conditions and different wind farm operating conditions.

The reduction in magnitude can be indirectly identified by sensing the voltage at the point before the step up transformer. This reduction can be used to identify faulted phases and estimate distance to fault.

### **8.3 Future Work**

With the system response analyzed in this research, a new protection scheme for protecting transmission lines connected to wind farms with Type 4 WTG was proposed. The wind farm collector feeder was not modeled, and the point of common coupling for the wind turbine was the point of interconnection to the transmission system. This research provided initial insight into the operating conditions of Type 4 wind turbines and their response to varied fault conditions and operating conditions. There are many issues that need to be looked into further to develop a protection scheme.

The following are some of the suggestions for follow-on research.

- Hardware implementation to determine the challenges when applied to physical power converters and WTGs.
- Evaluate performance with a realistic representation of a larger wind farm with step up transformers for every WTG, collector feeders, a collector substation and a station transformer

- Develop an algorithm to determine the ability of the relay to identify the voltage signal with fault impedance. Determine the influence of remote infeed from remote systems of varying.
- Develop a method to identify the faulted line for the case with multiple lines leaving the substation.
- Fault analysis with different combinations of nearly simultaneous faults to justify that the protection scheme works correctly.
- In this research, the grid is modeled as a Thevenin equivalent source behind impedance. To more clearly see the effect of the external system connected to the wind turbines, responses can be studied by integrating the WTG to system models with more detailed models of sources and loads.

## Appendix A – Test System Component Parameters

The system studied for this research is comprised of a Type 4 WTG system with a permanent magnet synchronous machine. The machine parameters and ratings are described in the following sections.

### A.1 Permanent Magnet Synchronous Machine (PMSM) ratings

Table A.1: Wind turbine (PMSM) generator ratings

Rated MVA	2 MVA
Rated Voltage	3.6 kV line-to-line
Rated frequency	60 Hz

### A.2 Permanent Magnet Synchronous Machine Parameters

Table A.2: Wind turbine (PMSM) generator per unit parameters[3].

Stator winding resistance	0.017 pu
Stator leakage reactance	0.064 pu
d-axis unsaturated reactance	0.55 pu
q-axis unsaturated reactance	1.11 pu
d-axis damper winding resistance	0.62 pu
d-axis damper winding reactance	0.183 pu
q-axis damper winding resistance	1.11 pu

q-axis damper winding reactance	1.175 pu
Magnetic Strength	1.0 pu

### A.3 Diode Bridge Rectifier

Each switch of the rectifier is a diode with the ratings given in Table A.3

Table A.3: Rectifier – diode ratings

Diode voltage rating	2.939 kV
Diode current rating	0.5 kA
RLC damping factor	0.9 pu
Base frequency of the system	60 Hz

### A.4 DC link capacitors

The parameters of the capacitors in the DC link are listed in Table A.4

Table A.4: DC link capacitor values

Capacitance	5400 $\mu$ F
Internal resistance	0.03 $\Omega$

The DC link is grounded in the midpoint of the two capacitors to provide a ground reference to the system, for avoiding the problem of a floating neutral.

The energy management system is discussed in the Chapter 5 is modeled as a capacitor bank whose capacitance is equal to 10 times the value of the DC link capacitors. The capacitors are connected through a bidirectional switch (bidirectional thyristors) which is turned on when the DC link voltage magnitude goes beyond 0.55pu.

### A.5 NPC Converter

Each switch of the NPC converter model is fired independently and separately within the operating conditions. The converter requires 6 diodes; these are modeled with the same ratings of the diodes in the machine side converter. The other switch ratings are as follows.

Table A.5: NPC converter switch ratings

Voltage rating	6.0 kV
Current rating	0.5 kA
RLC damping factor	0.9 pu
Base frequency of the system	60 Hz

### A.6 Low Pass Filter

The AC side filter used is a low pass L filter as shown in Figure 3.11(a). The filter will generally be an air core reactor, the inter-turn capacitance and turn-to-ground capacitance is also modeled, as those are the only paths for transients. The parasitic capacitance is modeled as a  $\pi$  branch putting together the inter-turn capacitance as a

single capacitor and turn-to-ground capacitance as two parallel branches at the beginning and end terminals of the reactor.

Table A.6: L filter values

Inductance	5 mH
Internal resistance	5 m $\Omega$
Turn to turn capacitance as a whole	3 nF
Turn to gnd capacitance as two branches	1 nF each

### A.7 Transformer

The transformer for a Type 4 WTGs will generally be a Delta-Star ground transformer and is modeled as 3 single phase transformers and connections are made accordingly.

The rating of each single phase transformer is as follows.

Table A.7: Transformer ratings

Primary Voltage	1.198 kV rms
Secondary Voltage	2.078 kV rms
Transformer MVA	0.733 MVA
Base frequency	60.0 Hz
Resistance	0.001 pu
reactance	0.15 pu

## A.8 Turbine Data

The turbine is modeled as a multi mass system with pitch control. The ratings of the turbine are as shown in Table A.8

Table A.8: Turbine Data

Rated Turbine power	2 MVA
Rated wind speed	12 m/s
Cut in wind speed	6.0 m/s
Cp	0.5176

## A.9 Controller

### A.9a High Pass Filter – Control Circuit

The time constant of the filter used in the controller is 0.002 sec. The gain is a scaling factor to convert the measured current values to pu.

The rated MVA and voltage values are 2 MVA and 3.6 kV LL respectively. The value of the rated current is calculated in equation (A.1)

$$I_{rated} = \frac{2MVA}{\sqrt{3} * 3.6kV} = 0.321 kA \quad (A.1)$$

The instantaneous current is measured, so as part of the conversion into pu value, it is divided by rated current times square root of two.

$$\frac{1}{0.321 * \sqrt{2}} = 2.205 \quad (A.2)$$

The transfer function of the filter is in the form of

$$G(j\omega) = \frac{1}{1+j\omega\tau} = Me^{j\phi} \quad (\text{A.3})$$

where M is the magnitude and  $\phi$  is the phase shift. To cancel  $G(j\omega)$ , a space vector is defined

$$I_{\alpha\beta} = I_{\alpha} + jI_{\beta} \quad (\text{A.4})$$

This, after filtering becomes

$$I_{F\alpha\beta} = Me^{j\phi}I_{\alpha\beta} \quad (\text{A.5})$$

Or in matrix form

$$\begin{bmatrix} I_{F\alpha} \\ I_{F\beta} \end{bmatrix} = \begin{bmatrix} M\cos\phi & -M\sin\phi \\ M\sin\phi & M\cos\phi \end{bmatrix} \begin{bmatrix} I_{\alpha} \\ I_{\beta} \end{bmatrix} \quad (\text{A.6})$$

The value of M and  $\phi$  are

$$M = \frac{1}{\sqrt{1^2 + (2\pi 60 * 0.002)^2}} = 0.798 \quad (\text{A.7})$$

$$\phi = -\tan^{-1}\left(\frac{2\pi 60 * 0.002}{1}\right) = -37.016 \text{ deg} \quad (\text{A.8})$$

To cancel the phase shift and magnitude we multiply by inverse of the matrix in equation (A.6)

$$T^{-1} = \frac{1}{0.798} \begin{bmatrix} \cos(-37.016) & -\sin(37.016) \\ \sin(37.016) & \cos(-37.016) \end{bmatrix} \quad (\text{A.10})$$

Simplifying the equation (A.10)

$$T^{-1} = \begin{bmatrix} 1 & -0.754 \\ 0.754 & 1 \end{bmatrix} \quad (\text{A.11})$$

The magnitude and phase shift can be cancelled by subtracting the d quantity by 0.754 times q quantity value and adding 0.754 times the d quantity value to the q quantity.

$$I_{d\_actual} = I_{d\_obtained} - 0.754 * I_{q\_obtained}$$

$$I_{q\_actual} = I_{q\_obtained} + 0.754 * I_{d\_obtained}$$

### A.9b Compensator

The gains for the PI compensator are calculated below.

The total inductance between the inverter terminals and point of interconnect is calculated as follows:

$$L_{tot} = L_{fil} + L_{trans} \quad (A.12)$$

$$L_{fil} = 5 \text{ mH} \quad (A.13)$$

$$L_{trans} = \frac{X_{pu} * \frac{V_{base}^2}{S_{base}}}{\omega} = 2.344 \text{ mH} \quad (A.14)$$

$$L_{tot} = 7.344 \text{ mH} \quad (A.15)$$

The total resistance in the series branch is

$$R_{tot} = R_{fil} + R_{trans} \quad (A.16)$$

$$R_{fil} = 5 \text{ m}\Omega \quad (A.17)$$

$$R_{trans} = R_{pu} * \frac{V_{base}^2}{S_{base}} = 5.8915 \text{ m}\Omega \quad (A.18)$$

$$R_{tot} = 0.0101 \Omega \quad (A.19)$$

The compensator gains are obtained by substituting these values in equations (3.17) and (3.18); the resistance of the switch is small and can be neglected.

$$K_p = \frac{L_{tot}}{\tau} = 1.46 \quad (\text{A.20})$$

$$K_i = K_p \frac{R_{tot}}{L_{tot}} = 2.178 \quad (\text{A.21})$$

### **A.10 Carrier signal**

The switching functions are generated by comparing the modulating waves with the carrier signal, which is a unipolar triangular signal with a frequency of 2 kHz.

## References

- [1] Amirnaser Yazdani and Reza Iravani: *Voltage-Sourced Converters in Power Systems – Modeling, Control, and Applications*. Wiley, March 2010.
- [2] G. Joós, “Wind Turbine Generator Low Voltage Ride through Requirements and Solutions.” *IEEE Power and Energy Society General Meeting*, 20 – 24 July, 2008.
- [3] Mohit Singh and Surya Santoso, *Dynamic Models for Wind Turbines and Wind Power Plants*. NREL and The University of Texas at Austin, October 2011
- [4] Antonio Luque, Olimpo Anaya-Lara, William Leithead and Grain P. Adam, “Coordinated control for wind turbine and VSC-HVDC transmission to enhance FRT capability.” *10<sup>th</sup> Deep Sea Offshore Wind R&D Conference*, Deep Wind’2013.
- [5] Rajveer Mittal, K. S. Sandhu and D. K. Jain, “Low Voltage Ride-Through of grid interfaced wind driven PMSG.” *Asian research publishing network* Vol. 4, No. 5 July 2009.
- [6] Rishabh Jain, *Grid Integrated Type 3 Wind Systems - Modeling, and Line Protection Performance Analysis using the RTDS*. Master’s Thesis, Dept of Electrical and Computer Engineering, University of Idaho, July 2014.
- [7] RTDS technologies. *Real time digital simulator controls library manual*, July 2013.
- [8] Remus Teodorescu, Marco Liserre and Pedro Rodriguez: *Grid Converters for Photovoltaic and Wind Power Systems*. Wiley, 2011.
- [9] Ankita Roy, *Protection performance study of a Type IV wind turbine system*. Master’s Thesis, Dept of Electrical and Computer Engineering, University of Idaho, December 2013.

- [10] Mohamed A. El-Sharkawi: *Electric Energy: An Introduction*, Third Edition. CRC Press, 2012.
- [11] Bing Chen ; Arun Shrestha, Fred A. Ituzaro, and Normann Fischer, "Addressing Protection Challenges Associated With Type3 and Type4 Wind Turbine Generators." presented at the 40th Annual Western Protective Relay Conference, October 2013.
- [12] N. Tleis, *Power System Modeling and Fault Analysis: Theory and Practice*. Newnes Power Engineering Series, 2008.
- [13] Dean Miller, "Fault Current Contributions from wind Plants." Proceedings of IEEE Power and Energy Society general meeting, San Diego, CA, 2012.
- [14] Pouyan Pourbeik, *Proposed Changes to the WECC WT4 Generic Model for Type 4 Wind Turbine Generators*. NREL, December 2011.
- [15] Reigh Walling, Ekrem Gursoy and Bruce English, "Current Contributions from Type 3 and Type 4 Wind Turbine Generators during Faults." *Transmission and Distribution Conference and Exposition (T&D)*, 2012 IEEE PES, 7-10 may, 2012.
- [16] D. Jovcic, Lisa Lamont and Keith Abbott, "Control system design for VSC transmission." *Electric Power Systems Research*, May 2007
- [17] J. R. Williams and B. Karlson, "Wind power plant short-circuit modeling guide," Sandia National Laboratories, New Mexico & California, SAND2012-6664, 2012
- [18] Wind Energy Basics [Online]. *Wind Energy Development Programmatic EIS*. <http://windeis.anl.gov/guide/basics/>
- [19] Magdi Ragheb and Adam M. Ragheb. *Wind Turbines Theory – The Betz Equation and optimal Rotor Tip Speed Ratio*. Available online at

<http://www.intechopen.com/books/fundamental-and-advanced-topics-in-wind-power/wind-turbines-theory-the-betz-equation-and-optimal-rotor-tip-speed-ratio>

- [20] *Wikipedia, Protective Relay for basics of Over current and distance relays*
- [21] J.L. Blackburn and T.J. Domin: *Protective Relaying: Principles and Applications, Fourth Edition*. CRC Press, 2014
- [22] S. M. Holder, Li Hang, B. K. Johnson, "Investigation of Transmission Line Protection Performance in an Electric Grid with Electronically Coupled Generation." *North American Power Symposium (NAPS)*, 2013, 22-24 September, 2013.